



Article

Understanding Changes in the Hydrometeorological Conditions towards Climate-Resilient Agricultural Interventions in Ethiopia

Satiprasad Sahoo ^{1,*} and Ajit Govind ²¹ International Institute of Geospatial Science & Technology (IIGST), Kolkata 700047, West Bengal, India² International Center for Agricultural Research in the Dry Areas (ICARDA), 2 Port Said, Victoria Sq, Ismail El-Shaer Building, Maadi, Cairo 11728, Egypt

* Correspondence: satisps@gmail.com

Abstract: Climate resilient agriculture (CRA) is very important to achieve long-term improvement in productivity and farm incomes under climate uncertainty. The present study focuses on investigating the plausible changes in the hydrometeorological conditions using big-data analysis techniques in the study of Ethiopia. The original contribution of this work envisages the importance of the CRA system in water-scarce areas for sustainable agriculture planning and management under changing climatic conditions. In the present research, a TerraClimate model was the basis for weather (precipitation and temperature) and hydrological data (runoff, actual evapotranspiration, potential evapotranspiration, vapor pressure deficit and climate water deficit); these data were used to determine the spatial distribution of the standardized anomaly index (SAI) and the slope of the linear regression for long-term (1958–2020) trend analysis. Future climate trend analysis (2021–2100) has been performed through the CMIP6 (EC-Earth3) shared socio-economic pathway (SSP 2) 4.5 dataset. Gravity Recovery and Climate Experiment (GRACE) with CSR and JPL data were utilized for the generation of water storage heat maps from 2002 to 2021. The results show that the average annual rainfall data for over 62 years was found to be 778.42 mm and the standard deviation is 81.53 mm. The results also show that the western part of the study area has the highest temperature trend, which diminishes as one moves eastward; the minimum temperature trend has been found in the western part of the study area. It was found that the equivalent water thickness (EWT) range of both CSR and JPL products was –15 to 40 cm. These results can help local climate-resilient development planning and enhance coordination with other institutions to access and manage climate finance.

Keywords: climate change; hydrological conditions; climate resilient agriculture; food security; GIS

Citation: Sahoo, S.; Govind, A. Understanding Changes in the Hydrometeorological Conditions towards Climate-Resilient Agricultural Interventions in Ethiopia. *Agronomy* **2023**, *13*, 387. <https://doi.org/10.3390/agronomy13020387>

Academic Editor: Xiangnan Li

Received: 20 December 2022

Revised: 25 January 2023

Accepted: 26 January 2023

Published: 28 January 2023



Copyright: © 2023 by the authors. Licensee MDPI, Basel, Switzerland. This article is an open access article distributed under the terms and conditions of the Creative Commons Attribution (CC BY) license (<https://creativecommons.org/licenses/by/4.0/>).

1. Introduction

Climate change due to greenhouse gas emissions is an indisputable fact worldwide and the average surface temperature will increase by 1.5 °C from 2030 to 2052 across the globe [1]. The food security problem is a major challenge worldwide. Agriculture is an economic activity and plays an important role in socio-economic development. However, climate-resilient agriculture (CRA) is very important for increasing agricultural productivity under climate variabilities from the local to global scale. Agricultural income can be reduced by 15–25% due to changing climatic conditions. Thus, CRA can reduce hunger and poverty to achieve long-term improved productivity. CRA is one type of composite approach including food security and components of agriculture directly affected by climate change. The World Bank promotes CRA as a “triple win” as follows: (i) enhanced productivity, (ii) resilience, and (iii) carbon sequestration.

There is strong statistical evidence that the climate is changing more quickly than expected, which will harm the economic development of developing countries as well as the general health of the community (Intergovernmental Panel on Climate Change) [2]. The

agricultural industry is one of several that will be adversely impacted by shifting rainfall patterns and rising temperatures [3]. The effects of climate change have a significant impact on farmers since they rely so much on agricultural activity. Therefore, farmers also need to know about the effects of climate change. Information about the climate is only valuable in mitigating the dangers caused by climate change when it is accessible in a way that smallholder farmers can comprehend [4]. Therefore, it is crucial to assess the major issues that prevent smallholder farmers from successfully utilizing weather information. Due to socioeconomic and political issues, a lack of adaptation ability, and several stresses of various sizes and sectors, Africa is especially susceptible to the dangers caused by climate change. The intense weather events, such as floods, droughts, and windstorms, which are brought on by climate change, have a substantial impact on food security in West Africa [5,6].

Ethiopia is now one of the nations most susceptible to climate change and fluctuation, regularly experiencing the effects of climate-related catastrophes, including floods and drought [7]. In the majority of Ethiopia, rain-fed agriculture is the primary means of growing crops. Therefore, the main causes of hunger and food scarcity are a lack of precipitation and the accompanying drought [8]. Precipitation is the main factor affecting agricultural activities in Ethiopia's northern region. Therefore, a significant influence on the quality of life for the inhabitants in this region is caused by a drop in rainfall [9]. Ethiopia has the poorest ability to adapt to climate change in Africa [10–13]. This is a result of dependence on rain-fed agriculture, poor water-supply infrastructure, rapid population growth, a lack of adaptability, shoddy organizations, and a lack of knowledge of environmental changes. In addition, Ethiopian mean annual temperatures are expected to rise by 0.9 to 1.1 °C by 2030, 1.7 to 2.1 °C by 2050, and 2.7 to 3.4 degrees Celsius by 2080, according to the International Panel on Climate Change [14]. During recent years, seasonal mean temperatures have increased in nations like Ethiopia [15]. Rising temperatures and volatility in rainfall will have an impact on the agricultural sector. The region's land use has seen a substantial alteration as a result of climatic variability. Therefore, changes in land use and the climate have a significant impact on hydrological processes [16–18]. Across all geographical and temporal dimensions, land use/land cover (LULC) change is one of the most significant contributors to changes in the land surface [19,20]. The change in land surface brought on by LULC has a profound influence on the hydrological processes [21–27]. Changes in LULC can affect terrestrial hydrology by changing the long-term equilibrium between rainfall and evapotranspiration [28]. Several earlier studies have demonstrated the impacts of LULC modification on runoff and evapotranspiration [19,22,23,26,29–33]. The runoff potential is significantly increased by the extension of agricultural land at the expense of plant cover [19,22,26,29,34]. Nevertheless, the features of the agro-ecological contexts of the research sites determine how much LULC or climatic fluctuations affect differences in runoff and evapotranspiration [29,30,35,36]. In Ethiopia's policy agenda, the sustainable use of water is gaining importance because this is one of the emerging nations where agricultural activity is the foundation of the economy, and where LULC-related natural issues pose significant problems to agriculture [37]. Therefore, a better understanding of how LULC influences watershed hydrology will enable local governments and policymakers to formulate and implement effective and appropriate response strategies.

Agriculture is the foundation of the economies of nations like Ethiopia. Water resources may be diminished as a result of agricultural operations, including flow management and irrigation techniques. As a result, the agricultural industry is now being impacted by drought caused by these issues [38,39]. Water and food availability are significant issues that mankind is currently experiencing due to an expanding population and continuous environmental issues [40]. It is crucial to research water availability so that people may determine if demand can be met by existing water sources [41]. In the management of water resources, the concept of water availability is strongly related to the more general idea of water sustainability [42]. Poor water management and the scarce availability of water for all users are caused by inadequate hydrological data [43]. Water resource expansion is

encouraged through appropriate management of sustainable water resources, and several methods have been developed to assess the sustainability of water resources [44]. The availability of water has substantially changed as a result of human and climate change [45]. In the context of an environment that is transforming, it is crucial to assess how sustainably distributed water resources are. An innovative method of assessing water resources is using satellite and global hydro-meteorological data. Also, a novel method of observing the water cycle has been made possible by the advancement of remote sensing technologies [46,47]. Information on a region's hydrological studies is provided through the Global Land Data Assimilation System (GLDAS) [48,49]. Additionally, the launch of the Gravity Recovery and Climate Experiment (GRACE) mission has made it possible to quantify TWS anomalies (TWSA) by recapturing temporal fluctuations in the Earth's gravity field at annual intervals [50]. GRACE data may be used to investigate the chronological evolution of the many components of the water cycle [51,52]. Thus, GRACE helps overcome the abovementioned limitations, and thus, it is widely used globally. GRACE was widely utilized by researchers to assess changes in groundwater or drought [53–55]. In places of the world with a lack of data, GRACE-derived outputs provide the potential of assessing groundwater degradation [56–58]. Through the use of GRACE data, groundwater monitoring work has been completed across Africa [59–61]. Water resources are affected by climate change in terms of how they are created, stored, and how quickly they are lost. These problems can be addressed with a climate-resilient agriculture (CRA) system. However, changes in CRA under changing climatic conditions raise these research questions:

- What are the predicted critical impacts of climate change on agricultural production?
- How do climate variables highly impact rainfed crop production and the livelihoods of subsistence farmers?
- What are the prime impacts that climate change is expected to have on agriculture in the Sahel region?
- How can we improve the resilience of countries' communities to present and future climate change?

Thus, there is a scope for the development of the CRA system under climate uncertainty. CRA is relevant to individual families who have independently established and developed without much investment from external funding. It can help to improve the livelihood strategies and attitudinal orientation of good owners. It can also improve the irrigation system for agriculture production in rural development to solve food security problems. The present research analyzes the spatiotemporal trend of past, present, and future climatic and hydrological conditions using big-data analysis techniques from Terra-Climate, CMIP6, GRACE, and GLDAS datasets for sustainable and efficient use of water resources in the era of climate uncertainty.

2. Materials and Methods

2.1. Study Area

Ethiopia is the nation where the study was carried out (Figure 1). Ethiopia's total area is 1,100,000 square kilometers. According to estimates, the population of Ethiopia is 117.88 million as of 2021. Ethiopia is the neighboring country of Sudan. The climate of Ethiopia varies mostly with height and ranges from the warm, dry lowlands to the chilly, wet plateau [62]. The country, which is located just north of the equator, has fairly constant temperatures all year long. Ethiopia's annual temperature ranges from 10.2 °C to 24.7 °C. The most recent regional climate prediction for Africa predicts that much of Ethiopia, sections of Eritrea, and Sudan will likely suffer drier than usual conditions. In 1984, there was a famine in Ethiopia, which resulted in starvation deaths of an estimated 1 million people. Due to its profound impact on the populations of a nation like Ethiopia, the drought situation is a serious issue. The economy of Ethiopia is heavily dependent on agriculture and the production of basic materials, typical of the majority of underdeveloped nations.

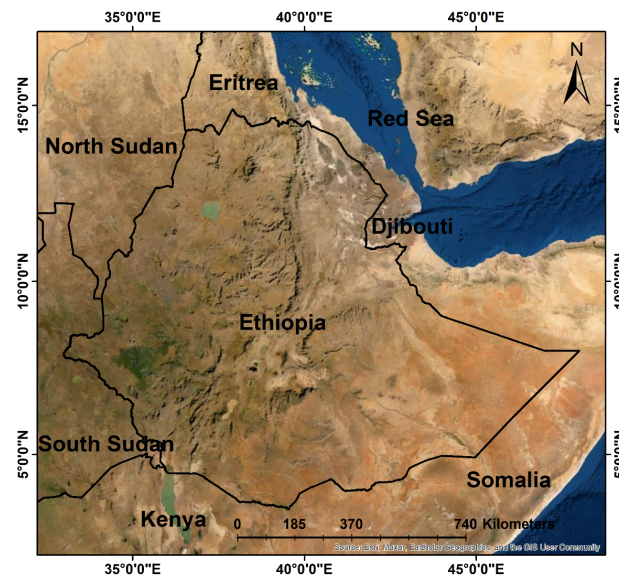


Figure 1. Ethiopia Map.

2.2. Data Used

The historical (1958–2020) climate (precipitation and temperature) and hydrological (runoff, actual evapotranspiration, potential evapotranspiration, vapor pressure deficit and climate water deficit) data were collected from the TerraClimate dataset (<https://www.climatologylab.org>, accessed on 23 October 2022). The future (2021–2100) climate [CMIP6 (EC-Earth3) Shared Socio-Economic Pathway (SSP 2) 4.5 data were collected from the NASA Center for Climate Simulation (<https://www.nccs.nasa.gov>, accessed on 23 October 2022). The GRACE of CSR and JPL data were collected from the Jet Propulsion Laboratory of the California Institute of Technology (<https://grace.jpl.nasa.gov>, accessed on 23 October 2022). The terrestrial water storage (TWS) and groundwater storage (GWS) data (2002–2021) were collected from the Global Land Data Assimilation System (<https://ldas.gsfc.nasa.gov>, accessed on 23 October 2022).

2.3. Methodology

In this study, climate (rainfall and temperature) and hydrological trend analysis have been performed based on the TerraClimate model dataset from 1958 to 2020. Using the non-parametric Mann–Kendall test, rainfall trend analysis was conducted for the selected research region. The Mann–Kendall test is used to see whether there are any patterns in the data series for both the yearly and monthly average rainfall. Then Sen’s slope estimator is used to calculate the magnitude of the trend. A regression model was devised for the observational rainfall data, which is the final step. The future climate trend analysis has been performed from the CMIP6 (EC-Earth3) SSP 2 4.5 dataset. The standardized anomaly index (SAI) and slope of the linear regression were used for the spatial distribution of climatic and hydrological conditions. The terrestrial water storage (TWS) and groundwater storage (GWS) scenarios have been generated based on the GRACE dataset from 2002 to 2021. The overall methodology is shown in Figure 2.

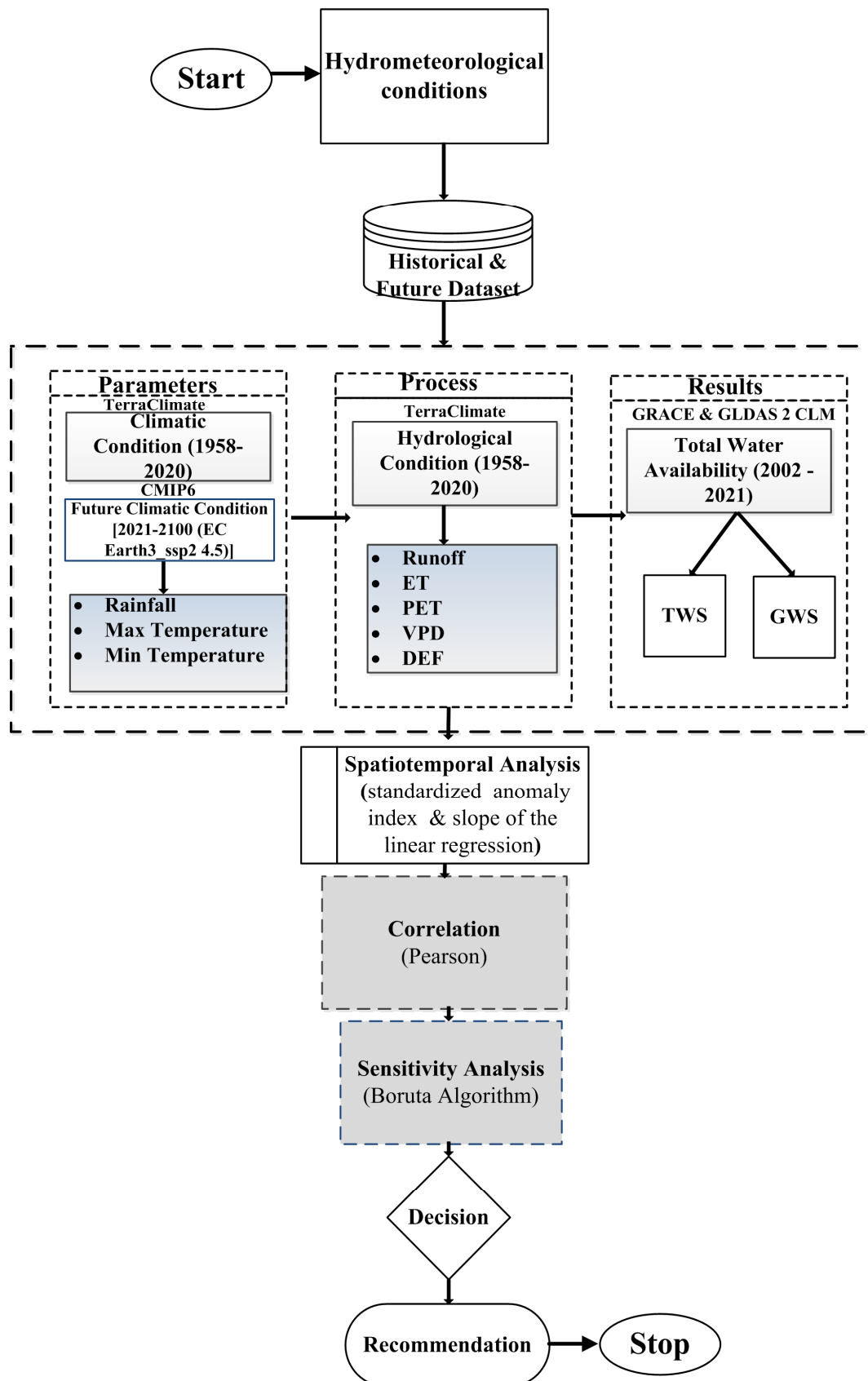


Figure 2. Overall methodological framework.

2.3.1. Mann–Kendall Test

The Mann–Kendall test is a non-parametric test because the normal distribution of time series data is not sensitive to this test [63]. The main use of this statistical model is the detection of patterns in time series of hydro-meteorological data.

$$S = \sum_{i=1}^{n-1} \sum_{j=i+1}^n \text{sign}(X_j - X_i) \quad (1)$$

where:

n = numbers of data points

X_j, X_i = annual values in years j ($i, j > 1$)

$\text{Sign}(X_j - X_i)$ has been calculated by using these equations

$$\text{sign}(X_j - X_i) = -1 \text{ for } (X_j - X_i) < 0 \quad (2)$$

$$\text{sign}(X_j - X_i) = 0 \text{ for } (X_j - X_i) = 0 \quad (3)$$

$$\text{sign}(X_j - X_i) = +1 \text{ for } (X_j - X_i) > 0 \quad (4)$$

The term “ $\text{sign}(X_j - X_i)$ ” refers to a specific sign capability that can accept the values [1, 0, or −1].

Depending on the magnitude of S , it may predict whether a trend will be declining or accelerating. A rising trend is indicated by a positive S value, and a declining trend is shown by a negative S value. At a 5% level of significance, a normalized test statistic is used to assess the statistical significance of the trend tendency of mean temperature and rainfall.

$$Z = \frac{n+1}{\sqrt{\text{var}(S)}} \text{ if } S > 0 \quad (5)$$

$$Z = 0 \text{ if } S = 0 \quad (6)$$

$$Z = \frac{n-1}{\sqrt{\text{var}(S)}} \text{ if } S < 0 \quad (7)$$

The degree of rainfall variability is assessed using the coefficient of variation (CV) (Hare, 2003). Additionally, the annual variation in rainfall and temperature was evaluated using the ANOVA test.

2.3.2. Sen’s Slope Estimator

For the purpose of identifying linear trends, simple linear regression is among the most commonly used models. However, this approach necessitates the presumption of residual normalcy [64]. Numerous hydrological variables do not follow a normal distribution as a result of the effect of natural occurrences. As a result, it was discovered that the Sen (1968) slope estimator is an effective tool for creating linear connections. Sen’s slope has an advantage over the regression slope in that it is less affected by large data series errors and outliers. A positive Sen’s slope reveals an upward tendency, whereas a downward trend is suggested by a negative Sen’s slope.

2.3.3. Linear Regression Analysis

One of the most popular techniques for finding patterns in data series is linear regression analysis [63]. It is a parametric model in which time is given as the independent variable and temperature and rainfall are regarded as the dependent variables. The correlation coefficient must be evaluated to determine the relationship between two variables, i.e., whether the two variables have a linear or non-linear relationship.

The linear regression equation is given as follows:

$$Y = mX + C \quad (8)$$

where, Y is the dependent variable, X is the independent variable, C is the intercept and m is the slope. Slope can help to determine how quickly changes in any kind of data.

The trend of the variable is defined by the sign of the slope. A positive slope indicates an increasing trend and a negative slope implies the line falls as y -axis increases.

2.3.4. Standardized Anomaly Index

A standardized anomaly index (SAI) is very important for spatial distributions of any kind of parameter to identify positive and negative trends for analysis purposes. SAI can be calculated as [65]:

$$SAI = \frac{(x - \mu)}{\sigma} \quad (9)$$

where, x is the yearly average, μ is the long-term average, and σ is the standard deviation.

2.3.5. Correlation and Sensitivity Analysis

A Pearson correlation coefficient was applied for hydrometeorological parameters to draw the relationship between the actual conditions. It is a measure of the linear correlation of variables; the value varies between -1 to 1 [66]. The sensitivity analysis has been performed with the Boruta algorithm (random forest classification) for hydrometeorological parameters to identify the importance of the dataset [67].

3. Results

3.1. Analysis of the Spatiotemporal Trend of Historical Climatic Conditions

One of the largest nations in Africa is Ethiopia. There is a significant fluctuation in temperature and precipitation because of its geographic position. The climate of Ethiopia is greatly manipulated by the migration of the Intertropical Convergence Zone (ITCZ) and related atmospheric circulation. The country's distinctive elevational and morphological variations are particularly efficient in regulating the local temperature. This explains why there is a variance in proximate local climates. This kind of regional climatic variance has a considerable influence on the region's agricultural activities. Agriculture is one of the key sectors for the economic growth of Ethiopia; it is facing numerous climate change related challenges due to low institutional and economic capacity. Especially floods and drought highly impact agricultural food systems, to leading food insecurity and malnutrition. This in turn contributes to an inability to build climate resilience for improved agricultural activity and food systems. In Ethiopia, irrigation and rain-fed agriculture account for the majority of agricultural activities, and one of the most important water sources for irrigation is groundwater. Groundwater supplies are significantly impacted by fluctuations in precipitation and temperature. This creates an uncomfortable situation in terms of the farmer's profits and limits spending on irrigation. These problems can be addressed with climate-resilient agriculture (CRA) and climate-smart agriculture (CSA) systems. It is necessary to maintain the stock of modern agricultural products, keeping the present and future agricultural system intact by keeping balance with nature.

In this research, the statistical analysis of the rainfall data for the study area from 1958 to 2020 has been discussed [Table S1]. The maximum and minimum annual rainfall have been determined to be 1029.45 mm and 585.29 mm, respectively (Table 1). Also, the average annual rainfall data for over 62 years was found to be 778.42 mm. The study area exhibits four seasons, namely: Bega, the long dry period from December to February; Belg, the long rainy period from March to May; Kiremt, the short dry spell from June to August; and Meher, the short rainy period from September to November. Belg and Meher are the two times of the year when grains are grown in Ethiopia. Rainfall patterns throughout the Belg season have a significant impact on the production of grains, which mostly comprise corn, wheat, sorghum, barley, and teff. The mean minimum rainfall of 11.21 mm has been recorded in Bega and the mean maximum rainfall of 299.91 mm has been recorded in Kiremt. The annual average rainfall has been calculated to be 778.42 mm and the standard deviation is 81.53 mm. The average rainfall for the Belg, Kiremt, Meher and Bega seasons has been determined to

be 191.44 mm, 446.97 mm, 92.43 mm, and 47.57 mm, respectively. Among the seasons, the greatest standard deviation was in the monsoon period and the lowest standard deviation was in the winter season. However, variability (coefficient of variance) has been calculated for every season; less variability has been recorded for monsoon rainfall and high variability has been recorded for winter rainfall. The ANOVA results concluded that the winter rainfall reduction had a high statistical significance ($F_{\text{Winter}} = 4.452$, $p < 0.01$).

Table 1. Mann–Kendall and Sen’s test for precipitation data of Ethiopia (1958–2020) [63,64].

	Min (mm)	Max (mm)	Mean (mm)	Standard Deviation (mm)	CV (%)	Correlation
Annual	585.29	1029.45	778.42	81.53	10.47379	−0.091
Belg	112.02	289.92	191.44	43.97	22.96981	0.03
Kiremt	244.7	475.42	354.66	45.3	12.77	−0.1
Meher	118.5	318.94	184.74	43.89	23.76	0.036
Bega	11.21	95.23	47.57	21.86	45.96211	−0.26

The Sen’s slope estimator, the Mann–Kendall test, and the regression model have been used to analyze the trend of rainfall data to develop the agricultural activities of the study area. Since both the Sen’s slope estimator and Kendall’s tau (Z) values were negative, the annual rainfall data trend is decreasing. For May, June, August, October, November, and December, a positive trend has been seen because Sen’s slope and Kendall’s tau (Z) values were both positive; the negative trend was for January, February, March, April, July, and September (Table 2).

Table 2. Monthly rainfall trend analysis results of Ethiopia (1958–2020) [63,64].

	Jan	Feb	Mar	April	May	June	July	Aug	Sep	Oct	Nov	Dec
Kendall’s tau	−0.16	−0.13	−0.067	−0.065	0.152	0.03	−0.153	0.107	−0.043	0.115	0.065	0.06
p-Value	0.06	0.11	0.4407	0.4406	0.07	0.73	0.07	0.21	0.61	0.18	0.45	0.48
Sen’s Slope	−0.11	−0.16	−0.09	−0.12	0.36	0.05	−0.28	0.16	−0.07	0.22	0.08	0.05

The linear regression analysis has been done for the annual precipitation data (Figure 2). The slope values show the trend rate of annual rainfall that is either increasing or decreasing. An increasing annual rainfall trend has been highlighted in the eastern part of Ethiopia and a decreasing annual rainfall trend has been observed in the western part of Ethiopia. In the northern portion of the study area, there is also evidence of an increasing trend in annual rainfall.

The western part of the study area has the highest temperature trend, which diminishes as one moves eastward; the minimum temperature trend was found in the western part of the study area (Figure 3). The results of the standardized precipitation anomaly index (SPAI) of Ethiopia have been shown in Figure 4. In 1960, the SPAI index varies from +0.87 to −1.57. Mild wetness has been designated as a condition in various portions of the northern, western, and southern parts of Ethiopia, and the central and northern parts of Ethiopia are in a dry condition. In 1970, the SPAI index varies from +2.30 to −1.27. Most of Ethiopia’s territory is in a dry condition, except for the western part, where there has been some mild wetness. In 1980, the SPAI index varies from +1.98 to −2.10. Except for some areas in the north, every region of Ethiopia has experienced great dryness during this time. In 1990, the SPAI index varies from +1.48 to −2.45.

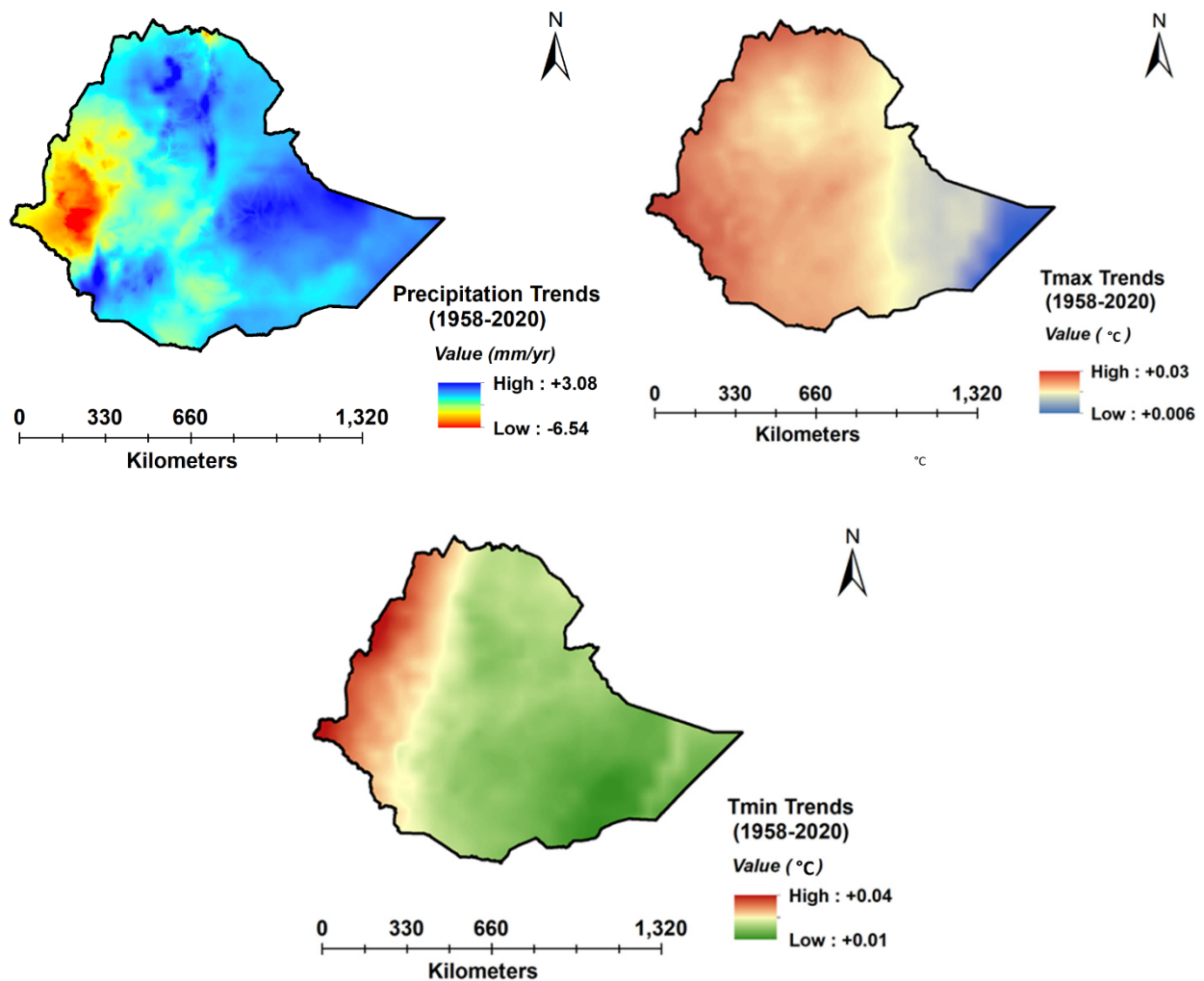


Figure 3. Spatial distribution of the precipitation, maximum and minimum temperature trend (slope of the linear regression) map for 1958–2020 in the study of Ethiopia.

The middle part, southern part, and some eastern parts of the study area were in moderate wet conditions. But the northern part faced extremely dry conditions during this period. In 2000, the SPAI index varies from +3.05 to −1.88. The southern region of Ethiopia has had great dryness throughout this time, whereas the northern region of the study area has seen extreme wetness. In 2010, the SPAI index varies from +2.31 to −2.46. The middle part of Ethiopia has been designated as in an extremely dry condition; an extremely wet condition has been found in the western part of Ethiopia. In 2020, the SPAI index varies from +6.88 to −2.86. Excessive dryness has had a substantial impact on the majority portion of Ethiopia. This is consistent with the results, which stated that Ethiopia's frequency of dry years has increased. Farmers' capacity to adapt to climate change and unpredictability would suffer from such annual variability issues with precipitation.

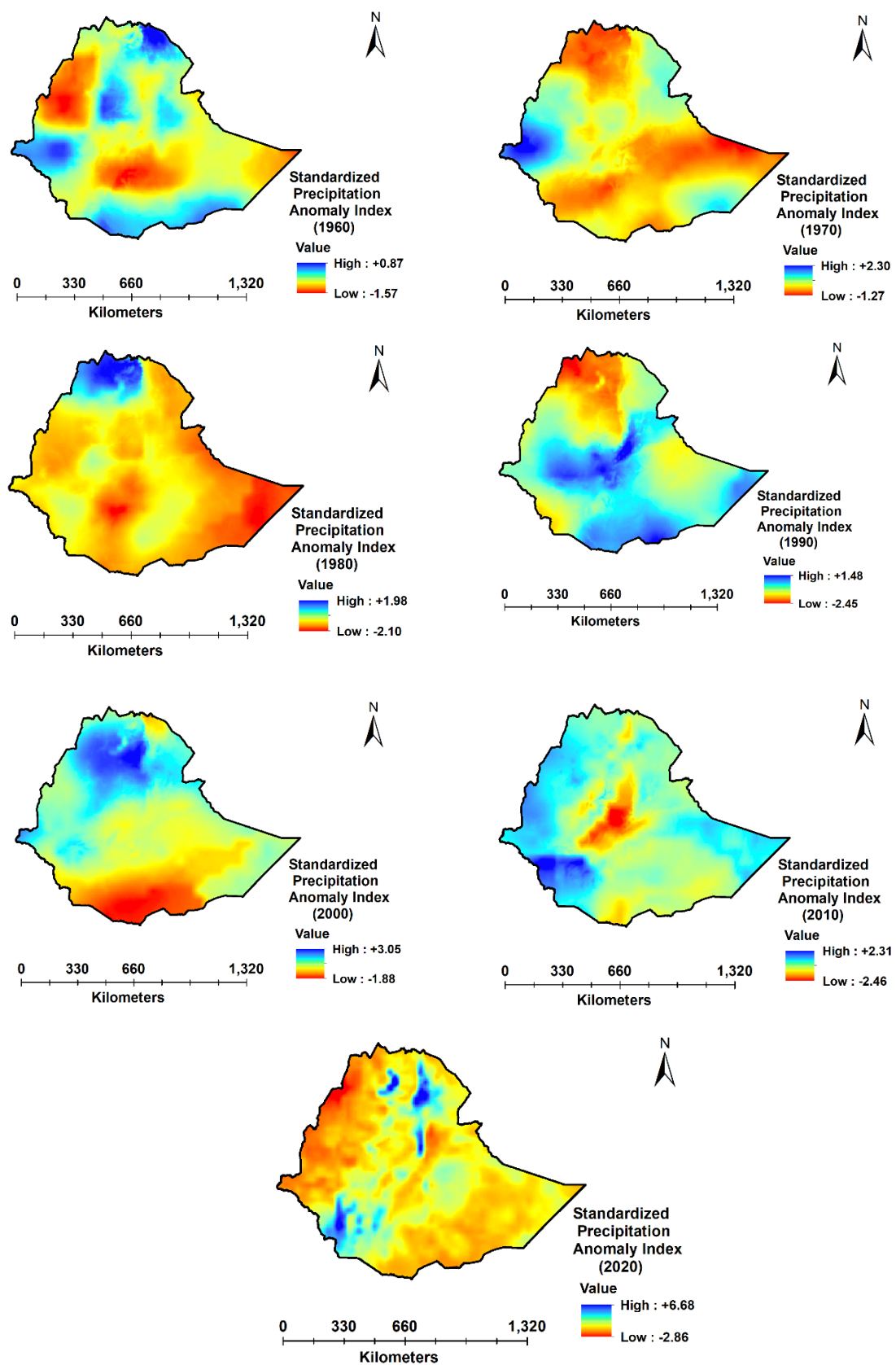


Figure 4. Standardized precipitation anomaly index maps for 1960, 1970, 1980, 1990, 2000, 2010, and 2020 in the study of Ethiopia.

Similarly, the IPCC (2014) reported that in the next few decades, due to global warming, drought, flooding, and precipitation unpredictability, there will be a danger of food poverty and the collapse of food systems. This places the country's impoverished inhabitants in an uncomfortable situation. The agricultural industry of Ethiopia will experience increased vulnerability due to the drought issue. Changes in rainfall patterns have caused several dilemmas for farmers. Certain crops have been cultivated in a specific season and within a particular rainfall range. As rain is the primary water source for agriculture in Ethiopia, the rate of production of seasonal crops is decreasing day by day due to changes in rainfall patterns and changes in rainfall quantity. Sometimes, the availability and variability of rainfall has an impact on families' capacity to take on risk and manage their liquidity.

There is also a link between rainfall patterns and the use of fertilizer. The availability of water and the frequency and quantity of fertilizer application are both influenced by the volume of rainfall. On the other hand, rainfall variability is to blame for raising the danger associated with fertilizer application because applying fertilizer under dry conditions might cause seedlings to burn and can elevate the chance that a crop will perish. The influence of temperature on agricultural productivity is significant. Plant productivity will be harmed by the predicted warming of the environment and the possibility of more drastic temperature occurrences. Farmers sometimes alter the seasonal crops they grow because of temperature changes. The temperature variation leads to changes in farmers' actions and choices, which have an impact on the exploitation of groundwater. Changes in weather and climate may have an oblique influence on groundwater collection by altering how arable land is used and how farming is conducted, which in turn affects how much water is available. Furthermore, higher temperatures may have a direct effect on how much water is available for agriculture. Hence, temperature variation has a crucial influence on the demand for water and irrigation equipment. The standardized anomaly index for minimum and maximum temperature have been further subjected to trend analysis (Figures 5 and 6).

However, climate variability directly impacts the vulnerability of the livestock industry in south-eastern Ethiopia. The higher number of cattle and sheep deaths was due to the pattern of increasing temperatures; the incidence and distribution of livestock diseases also increased. Thus, climate change is significantly affecting livestock production through ecosystem services. Therefore, climate change highly impacts plant and animal species, which respond either poleward or upslope. Thus, the grassland distribution is very important to control environmental factors because it is highly responsive to temperature, precipitation, and grazing pressure. The results show that poor grassland conditions are seen in the central plateau of Ethiopia due to high livestock density and adverse physical conditions. Sometimes, montane grassland has changed to evergreen thicket and scrub where the flat ground meets a steep slope.

Moreover, drought represents a significant constraint to crop cultivation. It causes periods of decreased production of essential crops and lower farmer incomes. This country is exposed to major climate risk for crop cultivation because heat stress will increase; this is due to the minimum temperature in the Belg season and high maximum and minimum temperatures in the Bega season. Thus, a large amount of groundwater is used for irrigation purposes. Groundwater management is a challenging task worldwide, especially in African countries because of the growing water demand for irrigation, and domestic, industrial, and ecosystem restoration. The aquifer storage and recovery (ASR) is a valuable tool for sustainable water supply depending on site-specific hydrogeological conditions. ASR projects are more applicable in areas that have high population density, changes in agriculture systems, massive dependence and increasing demand on groundwater for irrigation and domestic needs, and limited ground or surface water availability.

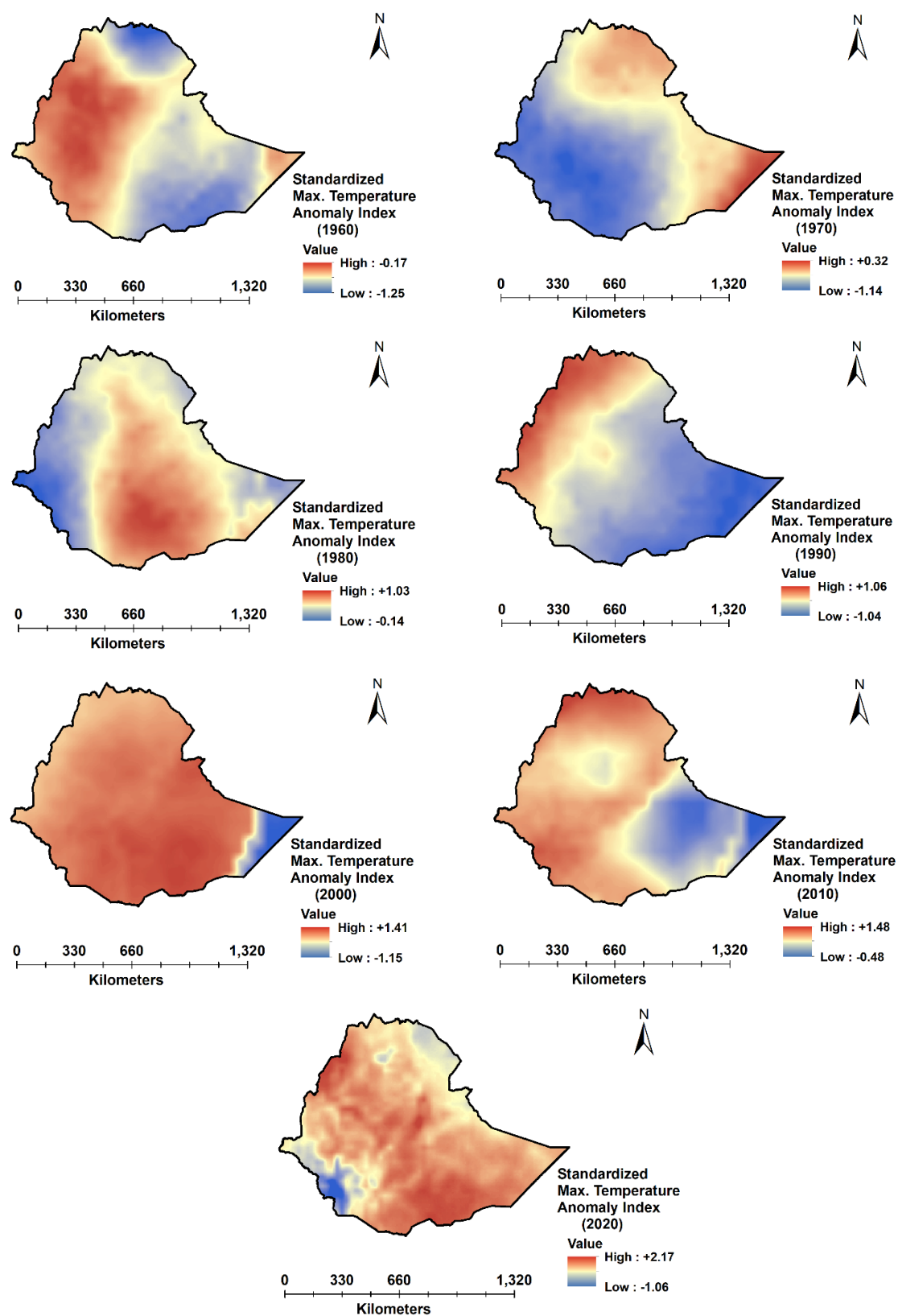


Figure 5. Standardized max. temperature anomaly index maps for 1960, 1970, 1980, 1990, 2000, 2010, and 2020 in the study of Ethiopia.

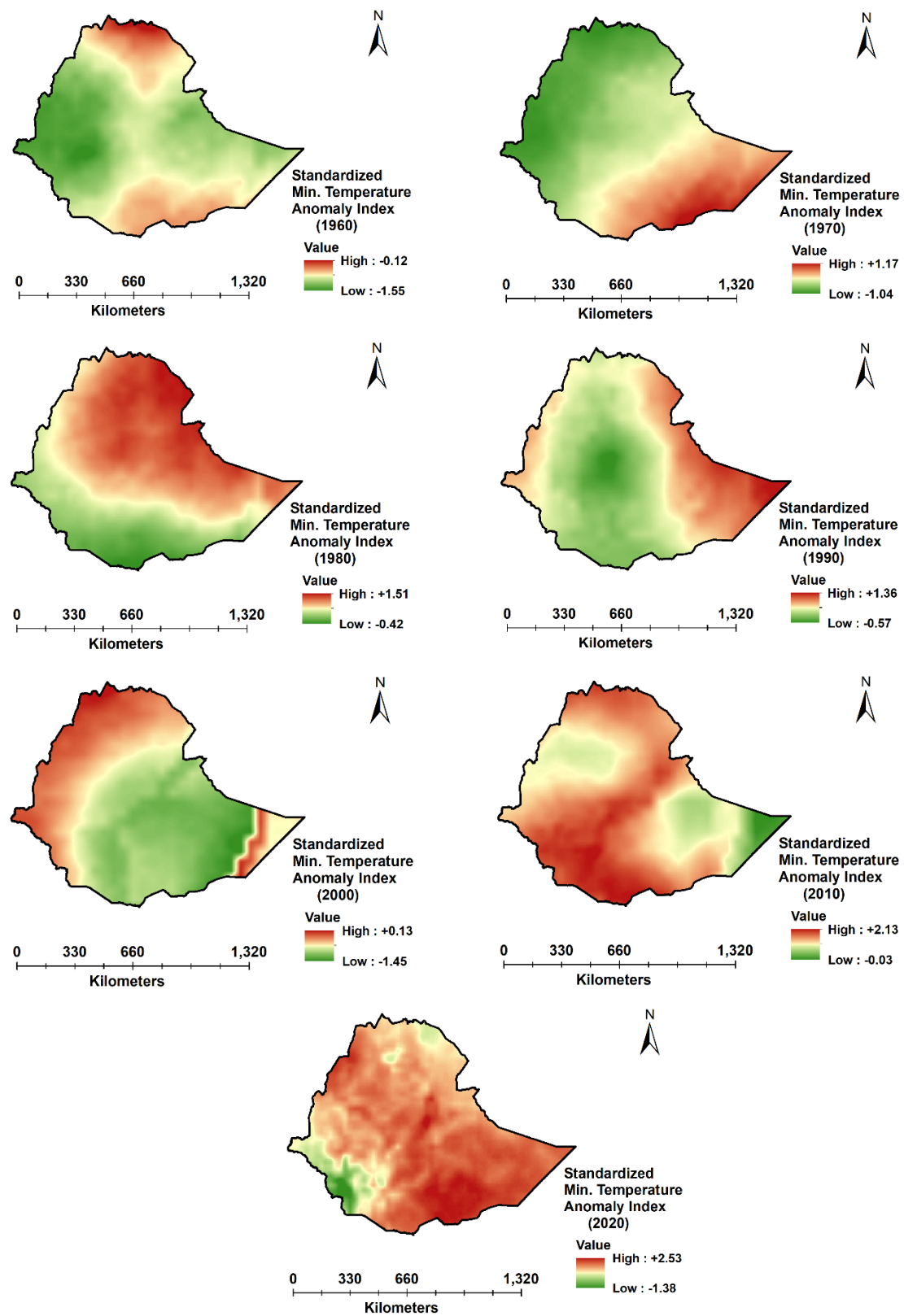


Figure 6. Standardized min. temperature anomaly index maps for 1960, 1970, 1980, 1990, 2000, 2010, and 2020 in the study of Ethiopia.

3.2. Analysis of the Spatiotemporal Trend of Future Climatic Conditions

Individual models can aid in a better understanding of variability among predicted climates, whereas multi-model ensembles provide the range and proportion of the most likely projected outcomes of change in the climate system for a chosen CMIP6 (EC Earth3) SSP2-4.5 [68]. The spatial distribution of the future precipitation and maximum and minimum temperature trend has been calculated by the slope of the linear regression technique from 2021 to 2100 (Figure 7). The results show that the northwestern part of the country has an increasing precipitation trend, and the northeastern and southeastern part has an increasing maximum and minimum temperature trend.

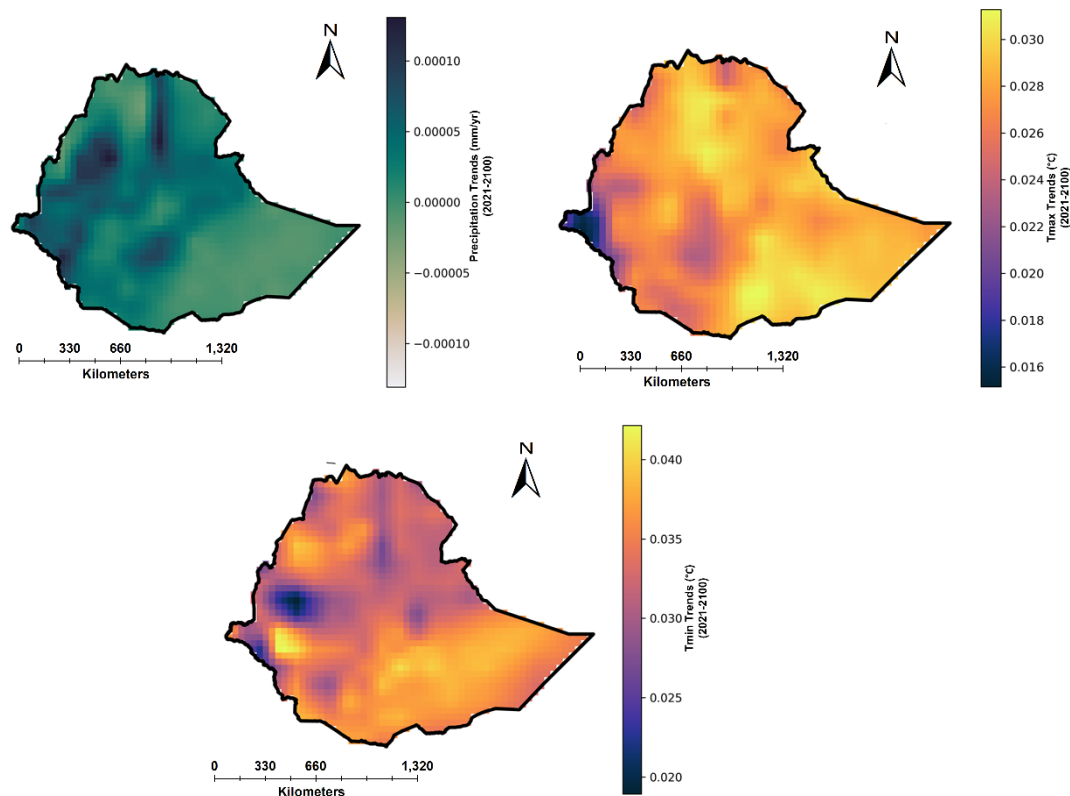


Figure 7. Spatial distribution of the future precipitation, maximum and minimum temperature trend (slope of the linear regression) map for 2021–2100 in the study of Ethiopia.

We also analyzed the future trends of climatic conditions in some important locations in this country. The average minimum and maximum annual temperatures in Tigray were found to be 16.62 °C and 31.01 °C, respectively. Between 2040 and 2059, Tigray's annual mean minimum and maximum temperatures were calculated to be 17.14 °C and 31.19 °C, respectively. The average minimum and maximum temperatures for Tigray were calculated to be 17.83 °C and 31.81 °C, respectively, between 2060 and 2079. In the years 2080–2099, Tigray's annual mean minimum and maximum temperatures were calculated at 18.27 °C and 32.28 °C, respectively. It was discovered that Tigray's estimated average annual precipitation would be 1101.92 mm from 2020 to 2039, 1230.31 mm from 2040 to 2059, 1229.29 mm from 2060 to 2079, and 1260.84 mm from 2080 to 2099. The minimum and maximum temperatures in Amhara each year are 13.98 °C and 28.18 °C, respectively. The calculated average minimum and maximum temperatures for Amhara between 2040 and 2059 were 14.48 °C and 28.43 °C, respectively. Amhara's average annual minimum and maximum temperatures were estimated to be 15.18 °C and 29.08 °C, respectively, between 2060 and 2079. The predicted average minimum and maximum temperatures for

Amhara from 2080 to 2099 were 15.67 °C and 29.49 °C, respectively. Amhara was estimated to receive 1363.32 mm of precipitation annually from 2020 to 2039, 1478.07 mm

from 2040 to 2059, 1452.34 mm from 2060 to 2079, and 1260.84 mm from 2080 to 2099. Benishangul Gumu's annual minimum and maximum temperatures were calculated to be 20.24 °C and 32.97 °C, respectively, during the years 2080–2099. The annual mean precipitation at Al Benishangul Gumu was derived as follows: 1232.68 mm from 2020 to 2039; 1422.71 mm from 2040 to 2059; 1414.31 mm from 2060 to 2079; and 1509.49 mm from 2080 to 2099. The mean minimum and maximum temperatures for the Oromia have been calculated to be 14.99 °C and 28.48 °C, respectively. From 2040 to 2059, the annual mean minimum and maximum temperatures in Oromia are calculated at 15.47 °C and 28.66 °C, respectively. The annual mean minimum and maximum temperatures in Oromia from 2060 to 2079 have been projected to be 16.12 °C and 29.29 °C, respectively. The annual mean minimum and maximum temperatures in the Oromia are forecasted to be 16.69 °C and 29.69 °C, respectively, from 2080 to 2099. Investigations have demonstrated that the Oromia region will receive 974.97 mm of mean precipitation from 2020 to 2039, 1048.42 mm from 2040 to 2059, 1089.64 mm from 2060 to 2079, and 1139.96 mm from 2080 to 2099. It has been calculated that from 2060 to 2079, the Gambela's mean annual minimum and maximum temperatures were 22.88 °C and 35.98 °C, respectively. Between 2080 and 2099, researchers discovered that the Gambela's mean annual minimum and maximum temperatures will be 23.40 °C and 36.27 °C, respectively. The annual mean minimum and maximum temperatures for SNNPR were calculated to be 16.92 °C and 31.29 °C, respectively, from 2020 to 2039. Between 2040 and 2059, SNNPR had yearly mean temperatures of 17.18 °C for the minimum and 31.19 °C for the maximum. Between 2060 and 2079, SNNPR's annual mean minimum and maximum temperatures were projected to be 17.81 °C and 31.72 °C, respectively. Between 2080 and 2099, SNNPR's annual mean minimum and maximum temperatures were predicted to be 18.31 °C and 32.04 °C, respectively. According to projections, the SNNPR will see annual mean precipitation totals of 733.43 mm from 2020 to 2039, 903 mm from 2040 to 2059, 898.69 mm from 2060 to 2079, and 959.05 mm from 2080 to 2099. It has been revealed that the Somali's annual minimum and maximum temperatures will be 20.47 °C and 33.36 °C, respectively, from 2020 to 2039. The annual mean minimum and maximum temperatures of the Somali were determined to be 21.15 °C and 33.76 °C, respectively, from 2040 to 2059; 21.81 °C and 34.42 °C, respectively, from 2060 to 2079; and 22.32 °C and 34.84 °C, respectively, from 2080 to 2099. The Somali's annual mean precipitation is predicted at 419.65 mm from 2020 to 2039, 479.35 mm from 2040 to 2059, 457.73 mm from 2060 to 2079, and 475.44 mm from 2080 to 2099. The Afar region is projected to have an annual mean temperature range between 18.73 °C and 32.28 °C from 2020 to 2039, 19.34 °C and 32.56 °C from 2040 to 2059, 20.04 °C and 32.29 °C from 2060 to 2079, and a range between 20.47 °C and 33.70 °C from 2080 to 2099. The annual mean precipitation in the Afar was projected to be 464.52 mm from 2020 to 2039, 582.89 mm from 2040 to 2059, 554.09 mm from 2060 to 2079, and 612.01 mm from 2080 to 2099.

In Afar and Amhara, the mean maximum and mean minimum temperatures throughout the summer in between 2020–2039 have been projected to be 36.27 °C and 14.19 °C, respectively. In Gambela and Amhara, the mean maximum and mean minimum temperatures throughout the winter have been projected to be 37 °C and 12.80 °C, respectively. In Afar and Amhara, the mean maximum and mean minimum temperatures throughout the summer in between 2040–2059 have been projected to be 36.40 °C and 14.76 °C, respectively. In Gambela and Amhara, the mean maximum and mean minimum temperatures throughout the winter have been projected to be 36.80 °C and 13.46 °C, respectively. In Afar and Amhara, in the period of 2060 to 2079, the mean maximum and mean minimum temperatures throughout the summer have been projected to be 36.91 °C and 15.36 °C, respectively. In Gambela and Amhara, the mean maximum and mean minimum temperatures throughout the winter have been projected to be 37.10 °C and 14.20 °C, respectively. In Afar and Amhara, in the period of 2080 to 2099, the mean maximum and mean minimum temperatures throughout the summer have been projected to be 37.03 °C and 15.82 °C, respectively. In Gambela and Amhara, the mean maximum and mean minimum temperatures throughout the winter have been projected to be 37.96 °C and 14.81 °C, respectively.

3.3. Analysis of the Spatiotemporal Trends of Historical Hydrological Conditions

The loss of water in a vapor state to the atmosphere from both the earth's surface and plants is known as evapotranspiration. A cropped soil's evapotranspiration is influenced by temperature, precipitation, and the amount of moisture that the soil can retain. This is the rationale for the introduction of the idea of actual evapotranspiration. An essential element of the hydrological cycle is actual evapotranspiration; it is one of the most important physical processes in natural ecosystems. It describes how water and energy are transferred between the soil, land surface, and atmosphere. The idea of actual evapotranspiration may be used to elucidate how worldwide climate change happens. So, the variability of climate change has a great impact on actual evapotranspiration. The most damaged ecosystems are those in Africa, which worsens the region's already acute water deficit. One of the largest nations in Africa is Ethiopia. There is a significant fluctuation in temperature and precipitation because of its geographic position. The climate of Ethiopia is greatly manipulated by the migration of the Intertropical Convergence Zone (ITCZ) and related atmospheric circulation. The country's distinctive elevational and morphological variations are particularly efficient in regulating the local temperatures. This explains why there is a variance in proximate local climates. This kind of regional climatic variance has a considerable influence on the region's hydrological processes. The geographical conditions impact actual evapotranspiration. So, an essential option for agricultural or hydrological investigations is the estimate of actual evapotranspiration.

The hydrological cycle's term for the potential evapotranspiration is also crucial for appropriate water management and efficient irrigation planning, which in turn has a big impact on crop water needs and water distribution. Potential evapotranspiration (PET) may be used for a variety of purposes, such as agricultural planning, drought monitoring, and assessing the impacts of global warming. Under specific climatic circumstances, PET may be thought of as the highest rate of evapotranspiration that can occur while soils or trees do not have a water shortage. It's important to comprehend both the actual evapotranspiration and PET to comprehend the crop's properties during the growing period. The eastward increase in annual actual evapotranspiration (AET) from -11.47 mm/yr in the west to -0.41 mm/yr in the east resembled the pattern of precipitation (Figure 8). The maximum trend of annual AET is found in the eastern part of Ethiopia and the minimum and moderate trends of annual AET have been found in the western and middle parts of Ethiopia.

Because erosion modifies the terrain, the runoff is crucial for research on how rivers evolve. Climate and biophysical factors have a big impact on runoff. Ethiopia is a tropical nation with a predominantly hilly terrain that is situated in the Horn of Africa. The rate of deforestation is considerable, and the mechanism for managing land use along the rugged terrain is ineffective. Land clearing has increased the quantity of runoff that occurs over the surface. The main cause of soil erosion is runoff. Nowadays, the primary financial and ecological concern for the whole world is soil degradation. In a country like Ethiopia, this type of soil erosion activity is becoming more prevalent every day. The result of the degradation of soil conditions is reduced crop output. Additionally, the research area's eastern, northern, and southern parts, have shown the highest annual runoff trend. As a result, these areas are seeing significant annual precipitation trends. The western and middle portion of the study area has the lowest and moderate annual runoff trends, which suggests that annual precipitation trends are modest. Additionally, the northeastern region, as well as a small fraction of the southern portion, have the highest trend of yearly potential evapotranspiration; a low trend in annual potential evapotranspiration has been identified for the center of Ethiopia. Some studies have proved the coherent relationship between potential evapotranspiration and actual evapotranspiration, which means it was anticipated that PET would rise, pushing AET to rise in tandem. As a result, it is anticipated that both changes will be synchronized.

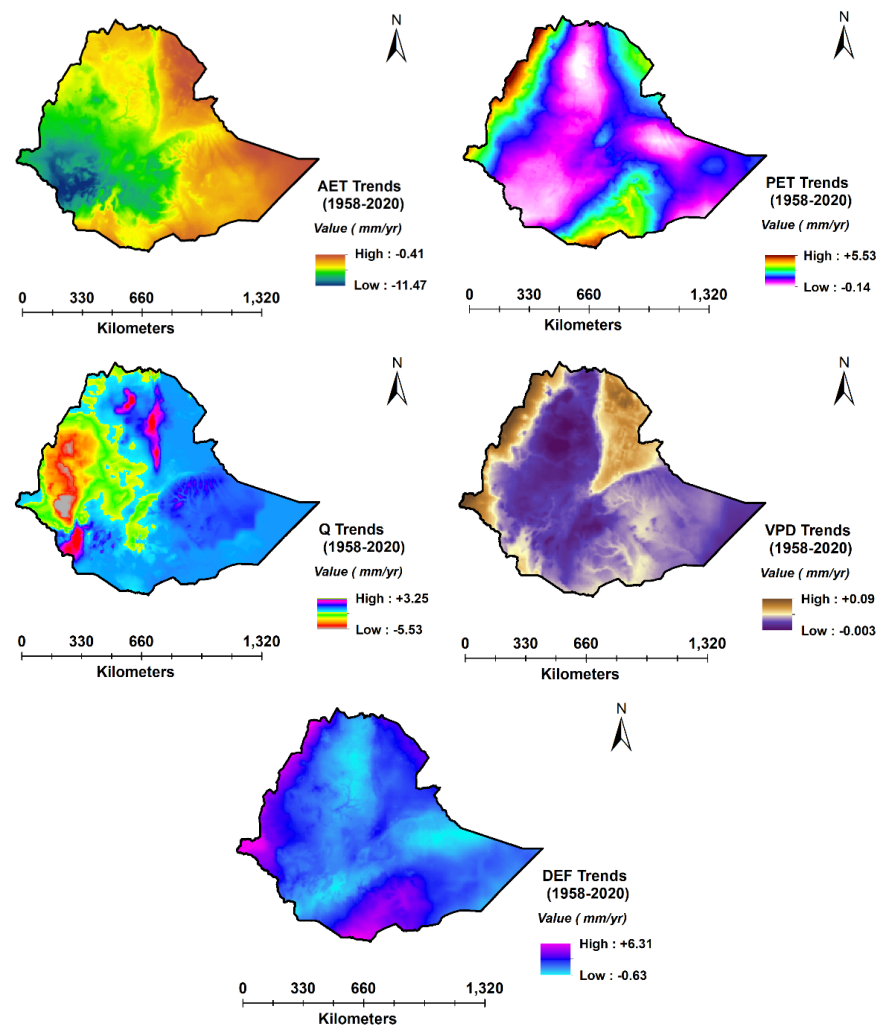


Figure 8. Spatial distribution of the AET, PET, Q, VPD and DEF trend (slope of the linear regression) map for 1958–2020 in the study of Ethiopia.

Given the shifting weather circumstances, the climate water deficit data shows the places that are under moisture stress. Water availability and need both have a role in the development of a plant water deficit. Rising temperatures can hasten the effects of water stress by creating a water shortage in the soil and atmosphere. Also, water stress in plants could be ameliorated by increasing the temperature. As a result of the shortage of water, plants are forced to deal with several diseases. Climate variability is frequently blamed for changes in forest cover, with periods of exceptionally warm and dry weather leading to decreased yearly leaf development. Temperature and rainfall readings are helpful determinants of climate change in any particular period. However, climatic water deficit helps to elucidate the climatic restriction on plant development, and this study may conclude the region's climatic conditions at a micro level. Climate is characterized as the interplay of water and energy, and the climatic water deficit (DEF), which is compounded as PET minus AET, monitors this relationship. When the amount of soil moisture accessible to plants to meet their evaporative needs is insufficient, this is indicated by high climatic water deficit values. Most of the regions of Ethiopia have a low trend of yearly climatic water deficits (Figure 8). In contrast, there has been a strong trend of climatic water deficit in various sections of the northeast and south. Modest annual climatic water deficits have been found in the northwest, north-east, and some southern part of the study area.

Another factor that is important to plants is the vapor pressure deficit (VPD), which depends on temperature and relative humidity. Instead of relative humidity, VPD is a more

precise approach to describe what causes a leaf to lose water. A high VPD means the air can absorb a large amount of water. Therefore, high VPD levels signify times of stomata. The air is almost saturated when the VPD is low and therefore, the plants are unable to transpire properly. The north-east and north-west regions of Ethiopia have a significant trend of yearly VPD and the plants can appropriately transpire in these areas (Figure 6). Ethiopia's center, eastern, and southern regions have had a low annual VPD trend.

3.4. Analysis of the Spatiotemporal Trends of Current Water Storage Conditions

The heat map of the monthly EWT describes the temporal variation in the GRACE data of the CSR and JPL for groundwater storage mechanisms at various study periods (2002–2021) in Ethiopia (Figure 9). The presented heat map has two axes, where the *x*-axis represents a yearly distribution of EWT and the *y*-axis is defined by the monthly distribution of EWT. The heat map images represent with different color intensities the varying EWT values recorded over an area during a period. The deep red color specifies high positive EWT indicating the months when water availability is higher than the mean for the study period, and vice versa for the blue.

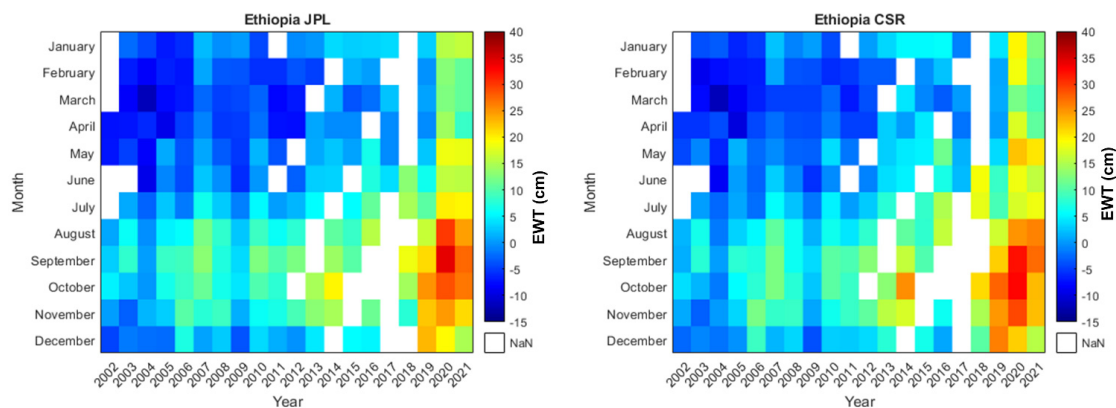


Figure 9. Monthly equivalent water thickness (EWT) variation from 2002 to 2021 obtained by GRACE [Center for Space Research (CSR) and Jet Propulsion Laboratory (JPL)] datasets on Ethiopia.

Both solutions CSR and JPL show almost similar patterns in the seasonal variability of EWT. The EWT range of both CSR and JPL products had -15 to 40 cm. In the early years, the water availability was below the mean level from January to June and above the mean level from July to December in the Ethiopia region. In recent years, the EWT gradually improved in this zone. For example, it was generally above the mean level in July to December during 2002–2018, similar to July–December in recent years (2019–2021) for the CSR data, while the JPL data had above the mean level in January–December in recent years (2019–2021). In addition, the lower mean level was in January–June 2002–2018 for the CSR, while the JPL found it in 2002–2017. From these results, water has become more available in recent years in the region. Though the outcomes of the two products were not consistent for this zone, both GRACE products exhibited an increase in red color in recent years, indicating a better EWT. For instance, the dynamics of the EWT maximum (August–September 2020, 40 cm) and minimum (March 2004, -15 cm) recorded for the JPL data were similar to the CSR retrieved maximum EWT of 40 cm in September–November 2020, and minimum recorded at -15 cm in March–April, during 2004 and 2005, respectively. A clearcut observation from the heat maps is that the historical years had a low availability of water during the monthly periods of January to June (2002–2018), whereas the recent years have an increasing trend of EWT during July to December (2002–2021), instead of more concentrated in 2020 and 2021 (August–October).

3.5. Analysis of the Spatiotemporal Trends of Current Terrestrial Water Storage Conditions

The highest and lowest TWS occurred in the year 2020 and 2017 (2338.55 mm and 319.01 mm, respectively) estimated by GLDAS 2.2 model [69]. The interannual TWS range value is found to be highest, at 1974.7 mm; and lowest, at 1881.3 mm, during 2016 and 2021, respectively (Figure 10). The central part of the area is concentrated with the medium TWS. The lowest TWS value was observed in the eastern part of the region, with the high TWS measured in the western part over all the years. However, the TWS level also followed a decreasing trend over the whole study region, from the western to the eastern part of the entire area. During the current period (2015–2021) the TWS was 2019.54 mm. However, it was observed that the minimum TWS followed an increasing trend during 2015–2017, then decreasing in the years 2018 to 2021.

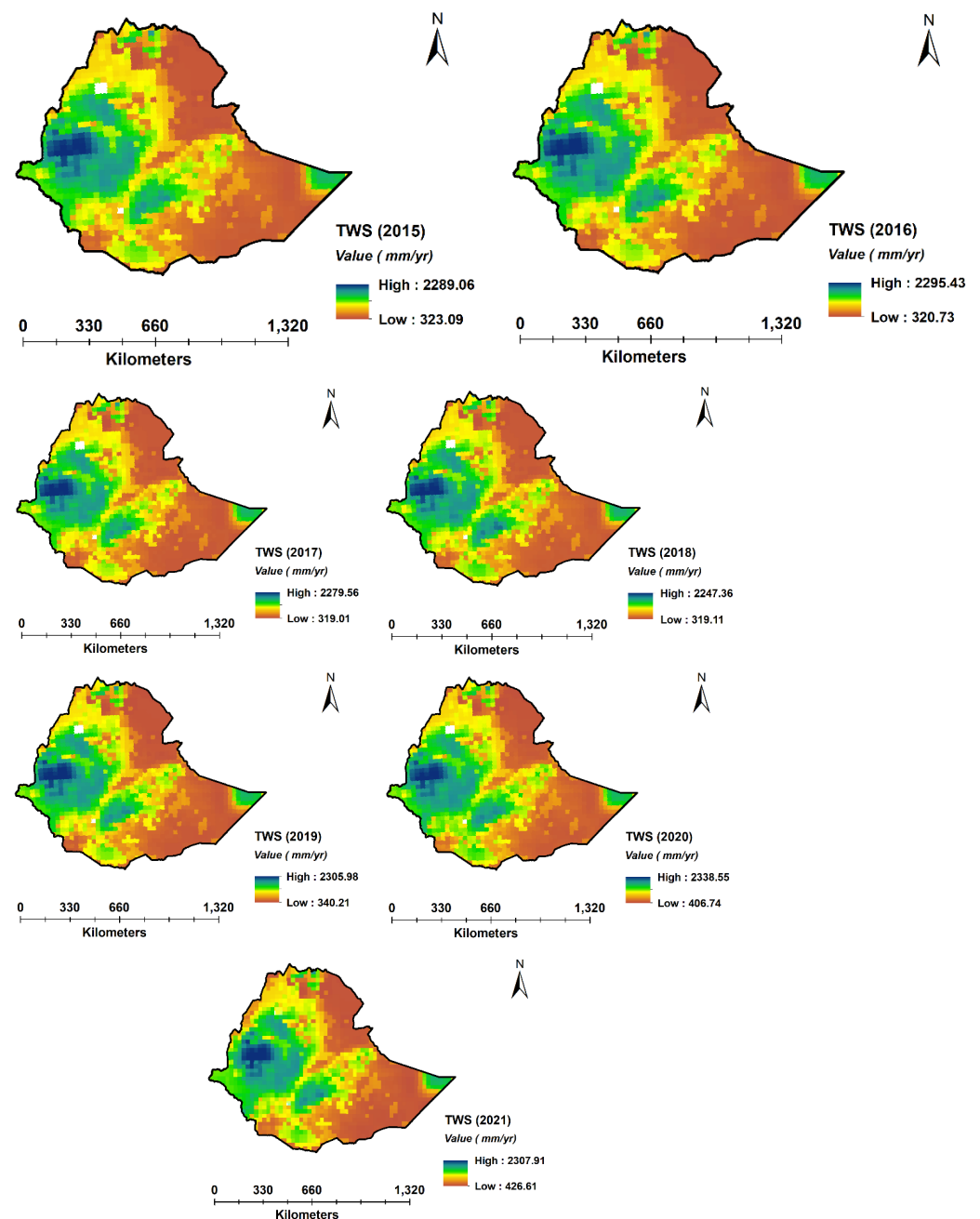


Figure 10. Annual terrestrial water storage (TWS) maps from GLDAS 2 CLM (2015–2021) in Ethiopia.

3.6. Analysis of the Spatiotemporal Trends of Current Groundwater Storage Conditions

The annual GWS variability is relatively maximal during 2020 (1952.02 mm), and minimal during 2018 (225.66 mm). However, this range of the GWS (1726.36 mm) was recorded during 2015–2021 (Figure 11). The inter-annual range of TWS variability is highest in 2016 (1690.333 mm), followed by 2015 (1679.67 mm), 2019 (1679.33 mm), 2017 (1677.35 mm), 2021 (1657.43 mm) and 2018 (1650.57 mm). The analysis shows that the variability of GWS in the studied region is high in the western part while low in the eastern part during the study period. Interestingly, the minimum TWS followed an increasing trend during most of the study period, except in 2015 and 2017.

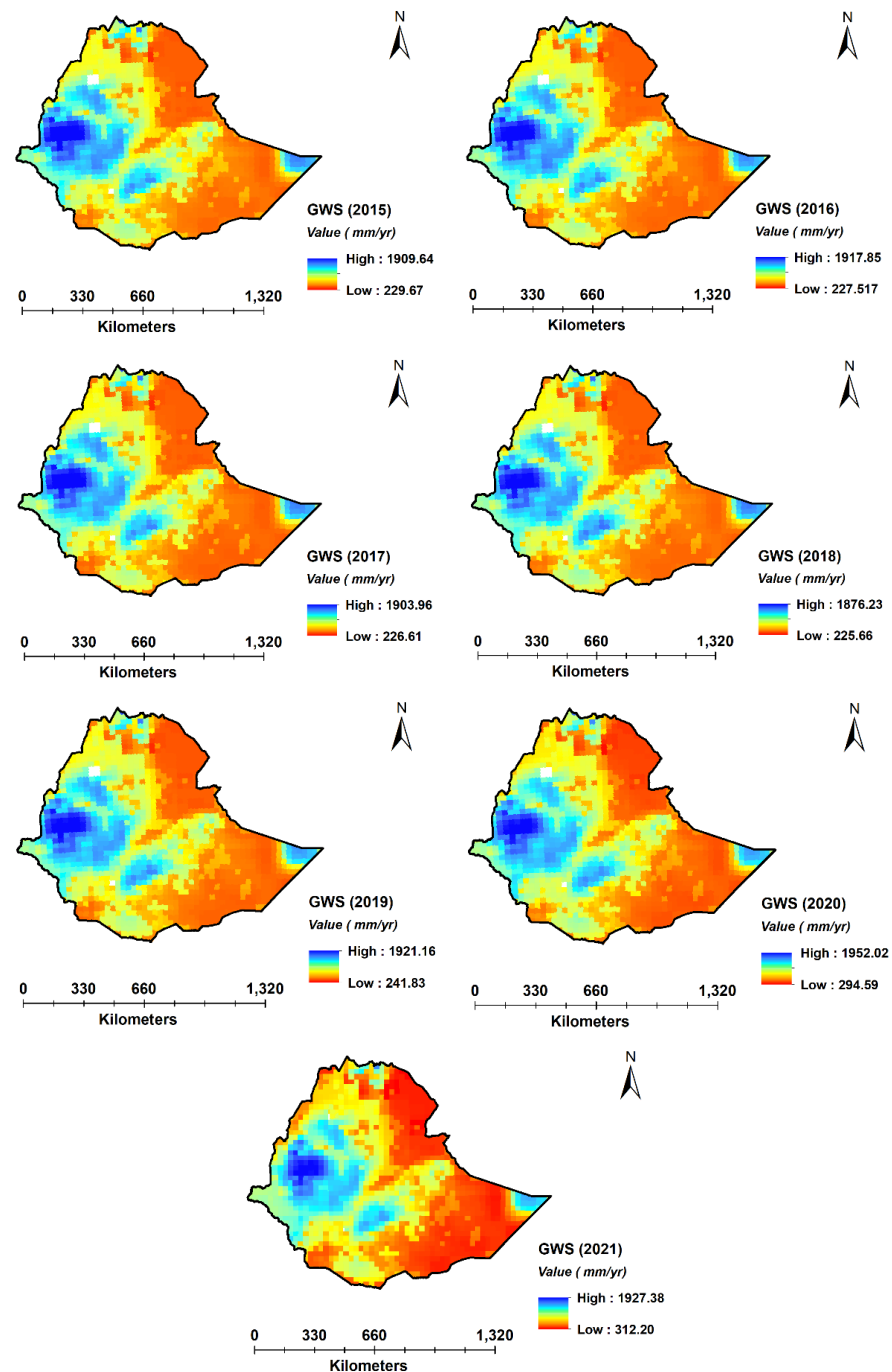


Figure 11. Annual groundwater storage (GWS) maps from GLDAS 2 CLM (2015–2020) in Ethiopia.

3.7. Correlation Analysis

Overall, the TWS presents strong negative correlations with the AET (−0.71), Q (−0.61), and VPD (−0.41) parameters, similarly, GWS showed strong negative correlations with the AET (−0.68), Q (−0.64) and VPD (−0.4) parameters, as well as an inverse relationship with the DEF (0.0012) indices only (Figure 12). The DEF presents a strong positive correlation with the PET (0.83) and VPD (0.67). The PPT shows a moderate negative correlation with the DEF (−0.45), Tmax (−0.52), Tmin (−0.44), and PET (−0.57), while showing a positive correlation with Q (0.55). Therefore, the correlation between TWS and GWS is robust (around 0.99), which is also evident from the analysis of spatial features.



Figure 12. Pearson correlation map of 2020 in Ethiopia.

3.8. Sensitivity Analysis

The Boruta algorithm was used to prioritize the selected factors affecting terrestrial water storage. The Boruta algorithm is built from the combined dataset using the random-forest classifier and performed in the BorutaPy library in Anaconda python [67].

The results of the Boruta method found the eight factors most important for the current study, namely, GWS, AET, Q, VPD, Tmin, PET, PPT, and DEF (Figure 13). Only the Tmax parameter was unimportant. According to the mean importance for the availability of terrestrial water storage, represented in Table 3, GWS (24.04) and AET (12.79), are the most important factors, followed by Q (9.50), VPD (8.01), Tmin (3.52), PET (2.79), PPT (2.81) and DEF (2.58). However, Tmax (0.35) was found to have no relevance among all considered factors.

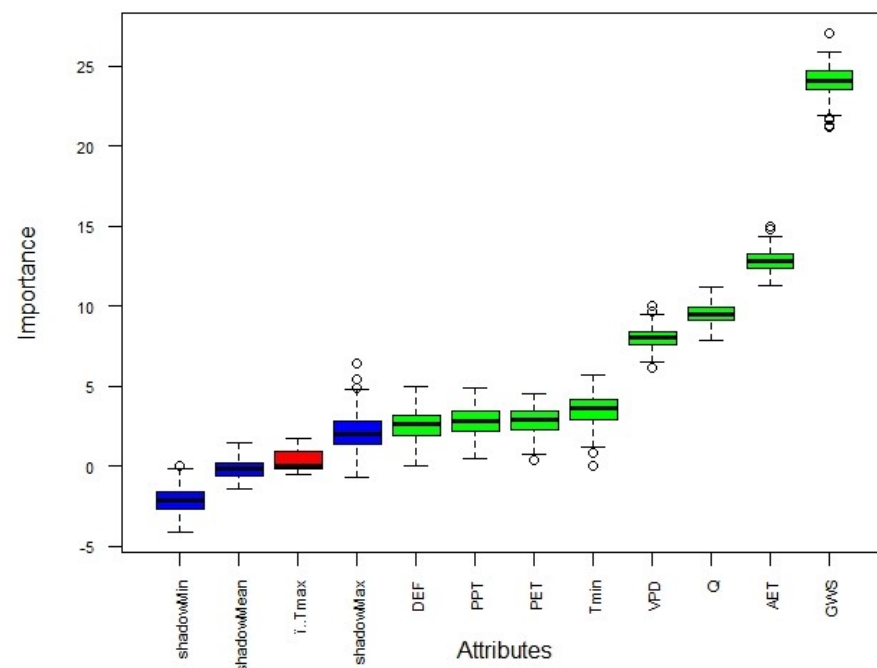


Figure 13. Terrestrial water storage variables importance using Boruta algorithm.

Table 3. Considering water storage variables importance using Boruta algorithm.

Parameters	Mean Importance	Median Importance	Min Importance	Max Importance	Decision
Tmax	0.35	−0.015	−0.55	1.75	Rejection
Tmin	3.52	3.59	0.05	5.72	Confirmed
AET	12.79	12.76	11.24	14.93	Confirmed
PET	2.79	2.87	0.33	4.51	Confirmed
VPD	8.01	8.02	6.17	10.01	Confirmed
Q	9.50	9.50	7.86	11.18	Confirmed
DEF	2.58	2.62	−0.007	4.97	Confirmed
GWS	24.04	24.08	21.19	27.03	Confirmed
PPT	2.81	2.84	0.47	4.87	Confirmed

4. Discussion

Climate change presents complex and interconnected risks; resilience is defined as the capacity to recover quickly from difficulties. The following elements are required: flexibility at a systematic level to respond to each situation, providing an improved adaptation investment strategy [70]. Flexible regulations, like renewable portfolio standards, low carbon fuel standards, and incorporating flexibility mechanisms are very significant to mitigate climate change [71]. Comprehensiveness, detail orientation, and quick decision-making are also very important. It helps to design climate services that are better tailored for climate change responses in particular contexts [72]. This can be understood from several perspectives, such as the restorative benefits to natural environments and the effectiveness of environmental education programs [73]. It is one of the important characteristics of resilience, with a potential for various applications in a social–ecological system [74]. The intentional duplication of system components and response pathways allows for partial failure within a system. Partial functional redundancy is a key expression of resilience in response to water insecurity [75]. These approaches are very important for planning, execution, and recovery [70]. This is the partnership that results when government, non-profit, private, and public organizations solve a problem that affects the whole community.

It is one type of organizational change that will be more successful when efforts are made to help people within an organization.

Climate resilient agriculture (CRA) mainly depends on changing climatic conditions. Climate change can disrupt food availability and quality. The different climatic conditions, such as changes in precipitation patterns, increase in temperatures and changes in extreme weather events, significantly impact agricultural productivity. Thus, future climatic conditions are very important for sustainable climate-resilient agriculture planning and management purposes. In the present research, CMIP6 (EC Earth3) SSP2-4.5 model was used for generating future scenarios of precipitation and temperature trends, up to the year 2100. One of our study locations shows the annual minimum and maximum temperatures in Benishangul Gumu were measured to be 18.69 °C and 32.11 °C, respectively. It was found that the annual minimum and maximum temperatures in Benishangul Gumu were projected to be 19.07 °C and 32.13 °C, respectively, between 2040 and 2059. Between 2060 and 2079, the annual minimum and maximum temperatures in Benishangul Gumu were projected to be 19.72 °C and 32.70 °C, respectively. The Gambela's mean minimum and maximum temperatures for the years 2020 to 2039 were projected to be 22.30 °C and 36.11 °C, respectively. The Gambela receives 798.30 mm of precipitation on average per year. It has been projected that from 2040 to 2059, the Gambela's mean annual minimum and maximum temperatures would be 22.40 °C and 35.64 °C, respectively. It was observed that rainfall availability is diminished for future planning purposes. Thus, climate-resilient technologies may face various constraints, such as limited knowledge of climate-resilient adaptation measures, an inadequate number of extension functions at the grassroots level, inadequate weather-based farm advisories, lack of knowledge about climate change, lack of reporting systems, and an inadequate number of automatic weather stations for respondents adapting to climate change. Thus, CRA is a very challenging issue for withstanding the shocks of climate change and extreme weather events. CRA practices must be flexible to tackle long-term climate change and also short-term weather events. The various cultural practices, such as proper preparatory cultivation, clean cultivation, adjusting planting/sowing/harvesting to avoid certain pests, balanced use of fertilizers, flooding the field, draining the field, alleyways, and harvesting of the crop can be highly maintained through modern techniques. Sustaining productivity can reduced the cost of cultivation and energy consumption. Therefore, these kinds of techniques are considered realistic solutions to the above-mentioned issues.

5. Climate-Resilient Agriculture and Development Practices

Adaptation in agriculture and development practices are essential for agricultural production resilience to climate change. Proper management and implementation of practice are required to increase agricultural production in unfavorable conditions to adapt to climate change. Some practices are given below that are followed at the rural level in Ethiopia:

5.1. Soil Resilience

Soil is the nexus of water, energy, and food. Sustainable soil management can be calculated from the response diversity of multi-omic markers [76]. Some essential factors, such as soil carbon, reducing erosion, and increasing the water retention capacity of the soil are required to improve resilience.

5.2. Adaptation in Crop Varieties

Adaptation in crop varieties refers to the relationship between environmental factors and the growth response of crop plants. It can help to reduce the negative impact of climate change on the agriculture system to ensure stable agricultural production. Introducing new crops leads to diversification of producing agriculture [77]. A few adaptations are required to improve crop varieties as follows: stakeholder participation and success; limiting factors are costs vs. benefits, legal aspects, implementation time, and lifetime.

5.3. Water Management

Water management is one of the major priorities in agricultural policy to prevent drought and build climate-resilient agriculture [78]. Agriculture is the largest source of livelihood for people in Ethiopia, where the gross domestic product (GDP) has been declining due to the rainfall deficit affecting crop production and farmers' incomes. Thus, water management strategies are required to improve drought mitigation, climate resilience, rainwater harvesting, and soil moisture management. It is also focused on canal irrigation, water use efficiency, and strategies for climate-resilient agriculture.

5.4. Conservation Tillage

Conservation tillage is a tillage system that involves the planting, growing, and harvesting of crops. It is very important for cover cropping, crop rotation, composting, and soil erosion control. It is often suggested as a resource-conserving alternative to increase crop productivity without compromising the soil health and cereal cropping system [79]. The various conservation tillage methods, such as zero-till, strip-till, ridge-till, and mulch till, can be used for soil cultivation that leaves the previous year's crop residue.

5.5. Farm Equipment Hiring

The low level of agricultural mechanization makes it very difficult to manage small and marginal farms [80]. Thus, modern farm equipment and technologies are essential to speed up planting/sowing and to deal with adverse events, such as erratic rainfall patterns.

5.6. Adaptation of Livestock Systems

The livestock system is very significant for the livelihood of two-thirds of rural communities. Adaptation of livestock systems is needed, such as a water reservoir, investing in heat-tolerant breeds, rotational grazing, and reduction in overgrazing, to enhance adaptation to heat stress and degradation. However, an integrated crop–livestock system can be productive and sustainable for a climate-resilient agriculture system [81].

6. Recommendations

Climate-Resilient Agriculture (CRA) is very significant for food security under changing climatic conditions. It can be helpful for the sustainable development of rural societies. The following recommendations should be advanced to ensure CRA for Ethiopia:

- Adaptation of appropriate mitigation technologies and agro-advisories for timely crop monitoring.
- Promote conservation agriculture and sustainable mechanization.
- Improved seed varieties that are adapted to be drought-resistant, heat-tolerant and flood tolerant.
- Crop insurance can be used as one of the strategies for CRA.
- Water smart technologies (furrow-irrigated raised bed, micro-irrigation, rainwater harvesting structure, cover-crop method, greenhouse, laser land leveling, reuse of wastewater, deficit irrigation, and drainage management) can help farmers to increase agriculture production under climate uncertainty.
- Adopting a good understanding of conjunctive use and artificial recharge, closely related to water resource management practices.
- To make the best use of surface water from wet periods and groundwater from dry periods for conjunctive use.
- To improve the understanding of how to build social inclusiveness into climate change response integration.
- Improved agriculture water data availability by open-source web service portal.
- Providing financial support for CRA projects.

7. Conclusions

In this study, the following objectives have been completed: to understand the long-term spatiotemporal trends for climatic (1958–2100), hydrologic (1958–2020), and water-storage (2002–2021) changes using TerraClimate, CMIP6, GRACE, and GLDAS datasets. The spatial distribution of the standardized anomaly index (SAI) and slope of the linear regression techniques was performed for climatic and hydrologic trend analysis purposes. CMIP6 (EC-Earth3) SSP 2 4.5 were utilized for future climate trend analysis. The GRACE of CSR and JPL and GLDAS 2 CLM data were used for EWT, TWS, and GWS analysis purposes. The correlation and sensitivity for hydrometeorological parameters was performed to identify the importance of and relationship between the actual conditions. The results show that the average rainfall for the Belg, Kiremt, Meher, and Bega seasons has been determined to be 191.44 mm, 446.97 mm, 92.43 mm, and 47.57 mm, respectively. It was noted that less variability has been recorded for monsoon rainfall and high variability has been recorded for winter rainfall. An increasing annual rainfall trend has been highlighted in the eastern part, and a decreasing annual rainfall trend has been observed in the western part of Ethiopia. It was found that the north-west part has an increasing future precipitation trend and the north-east and south-east parts have an increasing maximum and minimum future temperature trends. The concentration of a high vapor pressure deficit was in the central region; a high runoff trend result was shown for a small fraction of the upper and lower part of the region. The interannual terrestrial water storage (TWS) range value is found to be highest d (1974.7 mm) and lowest (1881.3 mm) during 2016 and 2021, respectively. The lowest TWS value was observed in the eastern part of the region, with a high TWS also measured in the western part. The analysis shows that the variability of GWS over the study region was high in the western part while low in the eastern part during the study period. It was observed that climate variability directly impacts the vulnerability of the livestock industry in south-eastern Ethiopia.

Moreover, these results can help local climate-resilient development planning and enhance coordination with other institutions to access and manage climate finance. This research also discusses climate-resilient agriculture and development practices for sustainable planning and management purposes. The recommendations also included for future development of the climate-resilient agriculture (CRA) system.

Supplementary Materials: The following supporting information can be downloaded at: <https://www.mdpi.com/article/10.3390/agronomy13020387/s1>, Table S1: Details of the monthly rainfall data for Ethiopia.

Author Contributions: Conceptualization, S.S., A.G.; methodology, S.S., A.G.; software, S.S., A.G.; validation, S.S., A.G.; formal analysis, S.S., A.G.; investigation, S.S., A.G.; resources, S.S., A.G.; data creation, S.S.; writing—original draft preparation, S.S., A.G.; writing—review and editing, S.S., A.G.; visualization, S.S.; supervision and revision, A.G., S.S.; project administration, A.G.; funding—A.G.; All authors have read and agreed to the published version of the manuscript.

Funding: This research was funded by CGIAR.

Institutional Review Board Statement: Not applicable.

Informed Consent Statement: Not applicable.

Data Availability Statement: We did not report any data, but data remains available upon request to the corresponding authors.

Acknowledgments: This work was carried out with support from the CGIAR Initiative on Climate Resilience, ClimBeR. We would like to thank the Belgium Federal Public Services (FPS) Foreign Affairs, Foreign Trade and Development Cooperation and all funders who supported this research through their contributions to the CGIAR Trust Fund (<https://www.cgiar.org/funders>, accessed on 23 October 2022) The author also thanks the International Center for Agricultural Research in the Dry Areas (ICARDA) for providing necessary support for this research work.

Conflicts of Interest: The authors declare no conflict of interest.

References

1. Zong, X.; Liu, X.; Chen, G.; Yin, Y. A deep-understanding framework and assessment indicator system for climate-resilient agriculture. *Ecol. Indic.* **2022**, *136*, 108597. [\[CrossRef\]](#)
2. Masson-Delmotte, V.; Zhai, P.; Pörtner, H.-O.; Debra Roberts, J.; Skea, I.; Shukla, P.R.; Pirani, A. *Global Warming of 1.5 °C; An IPCC Special Report on the Impacts of Global Warming*; IPCC: Geneva, Switzerland, 2018.
3. Dube, T.; Moyo, P.; Ncube, M.; Nyathi, D. The Impact of Climate Change on Agro-Ecological Based Livelihoods in Africa: A Review. *J. Sustain. Dev.* **2016**, *9*, 256. [\[CrossRef\]](#)
4. Muema, E.; Mburu, J.; Coulibaly, J.; Mutune, J. Determinants of access and utilisation of seasonal climate information services among smallholder farmers in Makueni County, Kenya. *Heliyon* **2018**, *4*, e00889. [\[CrossRef\]](#)
5. Sultan, B.; Gaetani, M. Agriculture in West Africa in the twenty-first century: Climate change and impacts scenarios, and potential for adaptation. *Front. Plant Sci.* **2016**, *7*, 1262. [\[CrossRef\]](#) [\[PubMed\]](#)
6. Sylla, M.B.; Pal, J.S.; Faye, A.; Dimobe, K.; Kunstmann, H. Climate change to severely impact West African basin scale irrigation in 2 °C and 1.5 °C global warming scenarios. *Sci. Rep.* **2018**, *8*, 14395. [\[CrossRef\]](#) [\[PubMed\]](#)
7. Rovin, K.; Hardee, K.; Kidanu, A. Linking population, fertility, and family planning with adaptation to climate change: Perspectives from Ethiopia. *Afr. J. Reprod. Health* **2013**, *17*, 15–29.
8. Admassie, A.; Adenew, B.; Tadege, A. Perceptions of stakeholders on climate change and adaptation strategies in Ethiopia. *IFPRI Res. Brief* **2018**, *15*, 2.
9. Tesfahunegn, G.B.; Mekonen, K.; Tekle, A. Farmers' perception on causes, indicators and determinants of climate change in northern Ethiopia: Implication for developing adaptation strategies. *Appl. Geogr.* **2016**, *73*, 1–12. [\[CrossRef\]](#)
10. Adem, A.; Amsalu, A. Assessment of climate change-induced hazards, impacts, and responses in the southern lowlands of Ethiopia. *Ethiop. J. Dev. Res.* **2012**, *34*, 1.
11. Conway, D.; Schipper, E.L.F. Adaptation to climate change in Africa: Challenges and opportunities identified from Ethiopia. *Glob. Environ. Chang.* **2011**, *21*, 227–237. [\[CrossRef\]](#)
12. Stige, L.C.; Stave, J.; Chan, K.S.; Ciannelli, L.; Pettorelli, N.; Glantz, M.; Herren, H.R.; Stenseth, N.C. The effect of climate variation on agro-pastoral production in Africa. *Proc. Natl. Acad. Sci. USA* **2006**, *103*, 3049–3053. [\[CrossRef\]](#)
13. Thornton, P.K.; Jones, P.G.; Alagarswamy, G.; Andresen, J.; Herrero, M. Adapting to climate change: Agricultural system and household impacts in East Africa. *Agric. Syst.* **2010**, *103*, 73–82. [\[CrossRef\]](#)
14. Oakes, T. *Climate Change 2007-Impacts, Adaptation and Vulnerability: Working Group II Contribution to the Fourth Assessment Report of the IPCC*; Cambridge University Press: Cambridge, UK, 2009.
15. Legesse, B.; Ayele, Y.; Bewket, W. Smallholder Farmers' Perceptions and Adaptation to Climate Variability and Climate Change in Doba District, West Hararghe, Ethiopia. *Asian J. Empir. Res.* **2013**, *3*, 251–265.
16. Li, Z.; Liu, W.; Zhang, X.C.; Zheng, F.L. Impacts of land use change and climate variability on hydrology in an agricultural catchment on the Loess Plateau of China. *J. Hydrol.* **2009**, *377*, 35–42. [\[CrossRef\]](#)
17. Mendes, J.; Maia, R. Hydrologic Modelling Calibration for Operational Flood Forecasting. *Water Resour. Manag.* **2016**, *30*, 5671–5685. [\[CrossRef\]](#)
18. Thapa, P. The Relationship between Land Use and Climate Change: A Case Study of Nepal. In *The Nature, Causes, Effects and Mitigation of Climate Change on the Environment*; IntechOpen: London, UK, 2021.
19. Bosch, J.M.; Hewlett, J.D. A review of catchment experiments to determine the effect of vegetation changes on water yield and evapotranspiration. *J. Hydrol.* **1982**, *55*, 3–23. [\[CrossRef\]](#)
20. Conway, D. The climate and hydrology of the Upper Blue Nile river. *Geogr. J.* **2000**, *166*, 49–62. [\[CrossRef\]](#)
21. Costa, M.H.; Botta, A.; Cardille, J.A. Effects of large-scale changes in land cover on the discharge of the Tocantins River, Southeastern Amazonia. *J. Hydrol.* **2003**, *283*, 206–217. [\[CrossRef\]](#)
22. Fang, X.; Ren, L.; Li, Q.; Zhu, Q.; Shi, P.; Zhu, Y. Hydrologic Response to Land Use and Land Cover Changes within the Context of Catchment-Scale Spatial Information. *J. Hydrol. Eng.* **2013**, *18*, 1539–1548. [\[CrossRef\]](#)
23. Gashaw, T.; Tulu, T.; Argaw, M.; Worqlul, A.W. Modeling the hydrological impacts of land use/land cover changes in the Andassa watershed, Blue Nile Basin, Ethiopia. *Sci. Total Environ.* **2018**, *619–620*, 1394–1408. [\[CrossRef\]](#)
24. Guo, H.; Bao, A.; Ndayisaba, F.; Liu, T.; Jiapaer, G.; El-Tantawi, A.M. De Maeyer, P. Space-time characterization of drought events and their impacts on vegetation in Central Asia. *J. Hydrol.* **2018**, *564*, 1165–1178. [\[CrossRef\]](#)
25. Woldesenbet, T.A.; Elagib, N.A.; Ribbe, L.; Heinrich, J. Hydrological responses to land use/cover changes in the source region of the Upper Blue Nile Basin, Ethiopia. *Sci. Total Environ.* **2017**, *575*, 724–741. [\[CrossRef\]](#) [\[PubMed\]](#)
26. Worku, S.; Derby, A.; Sinishaw, M.A.; Adem, Y.; Biadlegne, F. Prevalence of Bacteriuria and Antimicrobial Susceptibility Patterns among Diabetic and Nondiabetic Patients Attending at Debre Tabor Hospital, Northwest Ethiopia. *Int. J. Microbiol.* **2017**, *2017*, 5809494. [\[CrossRef\]](#)
27. Zhang, L.; Dawes, W.R.; Walker, G.R. Response of mean annual evapotranspiration to vegetation changes at catchment scale. *Water Resour. Res.* **2001**, *37*, 701–708. [\[CrossRef\]](#)
28. Garg, V.; Nikam, B.R.; Thakur, P.K.; Aggarwal, S.P.; Gupta, P.K.; Srivastav, S.K. Human-induced land use land cover change and its impact on hydrology. *HydroResearch* **2019**, *1*, 48–56. [\[CrossRef\]](#)
29. Dong, L.; Xiong, L.; Lall, U.; Wang, J. The effects of land use change and precipitation change on direct runoff in Wei River watershed, China. *Water Sci. Technol.* **2015**, *71*, 289–295. [\[CrossRef\]](#)

30. Li, G.; Zhang, F.; Jing, Y.; Liu, Y.; Sun, G. Response of evapotranspiration to changes in land use and land cover and climate in China during 2001–2013. *Sci. Total Environ.* **2017**, *596–597*, 256–265. [[CrossRef](#)] [[PubMed](#)]
31. Yang, X.; Ren, L.; Singh, V.P.; Liu, X.; Yuan, F.; Jiang, S.; Yong, B. Impacts of land use and land cover changes on evapotranspiration and runoff at Shalamulun River watershed, China. *Hydrol. Res.* **2012**, *43*, 23–37. [[CrossRef](#)]
32. Yin, J.; He, F.; Jiu Xiong, Y.; Yu, Q.G. Effects of land use/land cover and climate changes on surface runoff in a semi-humid and semi-arid transition zone in northwest China. *Hydrol. Earth Syst. Sci.* **2017**, *21*, 183–196. [[CrossRef](#)]
33. Zhang, Y.; Guan, D.; Jin, C.; Wang, A.; Wu, J.; Yuan, F. 2014. Impacts of climate change and land use change on runoff of forest catchment in northeast China. *Hydrol. Process.* **2014**, *28*, 186–196. [[CrossRef](#)]
34. Teklay, A.; Dile, Y.T.; Setegn, S.G.; Demissie, S.S.; Asfaw, D.H. Evaluation of static and dynamic land use data for watershed hydrologic process simulation: A case study in Gummara watershed, Ethiopia. *Catena* **2019**, *172*, 65–75. [[CrossRef](#)]
35. Guo, H.; Hu, Q.; Jiang, T. Annual and seasonal streamflow responses to climate and land-cover changes in the Poyang Lake basin, China. *J. Hydrol.* **2008**, *355*, 106–122. [[CrossRef](#)]
36. Ma, X.; Xu, J.; Luo, Y.; Prasad Aggarwal, S.; Li, J. Response of hydrological processes to land-cover and climate changes in Kejie watershed, south-west China. *Hydrol. Process. Int. J.* **2009**, *23*, 1179–1191. [[CrossRef](#)]
37. Dwivedi, R.S.; Sreenivas, K.; Ramana, K.V. Land-use/land-cover change analysis in part of Ethiopia using Landsat Thematic Mapper data. *Int. J. Remote Sens.* **2005**, *26*, 1285–1287. [[CrossRef](#)]
38. Jaramillo, F.; Destouni, G. Local flow regulation and irrigation raise global human water consumption and footprint. *Science* **2015**, *350*, 1248–1251. [[CrossRef](#)]
39. Winkler, K.; Gessner, U.; Hochschild, V. Identifying droughts affecting agriculture in Africa based on remote sensing time series between 2000–2016: Rainfall anomalies and vegetation condition in the context of ENSO. *Remote Sens.* **2017**, *9*, 831. [[CrossRef](#)]
40. Hao, Z.; AghaKouchak, A.; Nakhjiri, N.; Farahmand, A. Global integrated drought monitoring and prediction system. *Sci. Data* **2014**, *1*, 140001. [[CrossRef](#)]
41. Padowski, J.C.; Jawitz, J.W. Water availability and vulnerability of 225 large cities in the United States. *Water Resour. Res.* **2012**, *48*, 1–16. [[CrossRef](#)]
42. Barlow, P.M.; Alley, W.M.; Myers, D.N. Hydrologic Aspects of Water Sustainability and Their Relation to a National Assessment of Water Availability and Use. *Water Resour. Update* **2004**, *127*, 76–86.
43. Maliehe, M.; Mulungu, D.M.M. Assessment of water availability for competing uses using SWAT and WEAP in South Phuthiatsana catchment, Lesotho. *Phys. Chem. Earth* **2017**, *100*, 305–316. [[CrossRef](#)]
44. Maiolo, M.; Pantusa, D. Sustainable water management index, SWaM_Index. *Cogent Eng.* **2019**, *6*, 1603817. [[CrossRef](#)]
45. Prakash, S.; Gairola, R.M.; Papa, F.; Mitra, A.K. An assessment of terrestrial water storage, rainfall and river discharge over Northern India from satellite data. *Curr. Sci.* **2014**, *107*, 1582–1586.
46. Seyoum, W.M. Characterizing water storage trends and regional climate influence using GRACE observation and satellite altimetry data in the Upper Blue Nile River Basin. *J. Hydrol.* **2018**, *566*, 274–284. [[CrossRef](#)]
47. Yao, J.; Hu, W.; Chen, Y.; Huo, W.; Zhao, Y.; Mao, W.; Yang, Q. Hydro-climatic changes and their impacts on vegetation in Xinjiang, Central Asia. *Sci. Total Environ.* **2019**, *660*, 724–732. [[CrossRef](#)] [[PubMed](#)]
48. Rodell, M.; Houser, P.R.; Jambor, U.; Gottschalk, J.; Mitchell, K.; Meng, C.J.; Arsenault, K.; Cosgrove, B.; Radakovich, J.; Bosilovich, M.; et al. The Global Land Data Assimilation System. *Bull. Am. Meteorol. Soc.* **2004**, *85*, 381–394. [[CrossRef](#)]
49. Syed, T.H.; Famiglietti, J.S.; Rodell, M.; Chen, J.; Wilson, C.R. Analysis of terrestrial water storage changes from GRACE and GLDAS. *Water Resour. Res.* **2008**, *44*, 1–15. [[CrossRef](#)]
50. Wahr, J.; Molenaar, M.; Bryan, F. Time variability of the Earth’s gravity field’ Hydrological and oceanic effects and their possible detection using GRACE. *J. Geophys. Res. Solid Earth* **1998**, *103*, 30205–30229. [[CrossRef](#)]
51. Chen, J.L.; Wilson, C.R.; Tapley, B.D. The 2009 exceptional Amazon flood and interannual terrestrial water storage change observed by GRACE. *Water Resour. Res.* **2010**, *46*, 1–10. [[CrossRef](#)]
52. Ramillien, G.; Frappart, F.; Güntner, A.; Ngo-Duc, T.; Cazenave, A.; Laval, K. Time variations of the regional evapotranspiration rate from Gravity Recovery and Climate Experiment (GRACE) satellite gravimetry. *Water Resour. Res.* **2006**, *42*, 1–8. [[CrossRef](#)]
53. Li, T.; Zhang, Q.; Zhao, Y.; Gao, Y. Detection of groundwater storage variability based on GRACE and CABLE model in the Murray-Darling Basin. *E3S Web Conf.* **2019**, *131*, 1067. [[CrossRef](#)]
54. Mo, X.; Wu, J.J.; Wang, Q.; Zhou, H. Variations in water storage in China over recent decades from GRACE observations and GLDAS. *Nat. Hazards Earth Syst. Sci.* **2016**, *16*, 469–482. [[CrossRef](#)]
55. Shamsudduha, M.; Taylor, R.G.; Jones, D.; Longuevergne, L.; Owor, M.; Tindimugaya, C. Recent changes in terrestrial water storage in the Upper Nile Basin: An evaluation of commonly used gridded GRACE products. *Hydrol. Earth Syst. Sci.* **2017**, *21*, 4533–4549. [[CrossRef](#)]
56. Wang, X.; De Linage, C.; Famiglietti, J.; Zender, C.S. Gravity Recovery and Climate Experiment (GRACE) detection of water storage changes in the Three Gorges Reservoir of China and comparison with in situ measurements. *Water Resour. Res.* **2011**, *47*, 1–13. [[CrossRef](#)]
57. Forootan, E.; Rietbroek, R.; Kusche, J.; Sharifi, M.A.; Awange, J.L.; Schmidt, M.; Omondi, P.; Famiglietti, J. Separation of large scale water storage patterns over Iran using GRACE, altimetry and hydrological data. *Remote Sens. Environ.* **2014**, *140*, 580–595. [[CrossRef](#)]

58. Rodell, M.; Chen, J.; Kato, H.; Famiglietti, J.S.; Nigro, J.; Wilson, C.R. Estimating groundwater storage changes in the Mississippi River basin (USA) using GRACE. *Hydrogeol. J.* **2007**, *15*, 159–166. [\[CrossRef\]](#)
59. Awange, J.L.; Gebremichael, M.; Forootan, E.; Wakbulcho, G.; Anyah, R.; Ferreira, V.G.; Alemayehu, T. Characterization of Ethiopian mega hydrogeological regimes using GRACE, TRMM and GLDAS datasets. *Adv. Water Resour.* **2014**, *74*, 64–78. [\[CrossRef\]](#)
60. Kenea, T.T.; Kusche, J.; Kebede, S.; Güntner, A. Forecasting terrestrial water storage for drought management in Ethiopia. *Hydrol. Sci. J.* **2020**, *65*, 2210–2223. [\[CrossRef\]](#)
61. Saber, M.; Kantoush, S.A.; Sumi, T. Assessment of spatiotemporal variability of water storage in Arabian countries using global datasets: Implications for water resources management. *Urban Water J.* **2020**, *17*, 416–430. [\[CrossRef\]](#)
62. Abebe, T. Climate change National Adaptation Programme of Action (NAPA) of Ethiopia. *Glob. Environ. Facil.* **2007**, *2*, 96.
63. Gadedjisso-Tossou, A.; Adjegan, K.I.; Kablan, A.K.M. Rainfall and temperature trend analysis by Mann–Kendall test and significance for rainfed cereal yields in Northern Togo. *Science* **2021**, *3*, 17. [\[CrossRef\]](#)
64. McBean, E.; Motiee, H. Assessment of impact of climate change on water resources. *Hydrol. Earth Syst. Sci.* **2008**, *12*, 239–255. [\[CrossRef\]](#)
65. Dutta, D.; Kundu, A.; Patel, N.R.; Saha, S.K. Siddiqui, A.R. Assessment of agricultural drought in Rajasthan (India) using remote sensing derived Vegetation Condition Index (VCI) and Standardized Precipitation Index (SPI). *Egypt. J. Remote Sens. Space Sci.* **2015**, *18*, 53–63.
66. Yang, H.; Luo, P.; Wang, J.; Mou, C.; Mo, L.; Wang, Z.; Bhatta, L.D. Ecosystem evapotranspiration as a response to climate and vegetation coverage changes in Northwest Yunnan, China. *PLoS ONE* **2015**, *10*, e0134795. [\[CrossRef\]](#)
67. Ahmed, A.M.; Deo, R.C.; Feng, Q.; Ghahramani, A.; Raj, N.; Yin, Z.; Yang, L. Deep learning hybrid model with Boruta-Random forest optimiser algorithm for streamflow forecasting with climate mode indices, rainfall, and periodicity. *J. Hydrol.* **2021**, *599*, 126350. [\[CrossRef\]](#)
68. Bilbao, R.; Wild, S.; Ortega, P.; Acosta-Navarro, J.; Arsouze, T.; Bretonnière, P.A.; Vegas-Regidor, J. Assessment of a full-field initialized decadal climate prediction system with the CMIP6 version of EC-Earth. *Earth Syst. Dyn.* **2021**, *12*, 173–196. [\[CrossRef\]](#)
69. Sahoo, S.; Chakraborty, S.; Pham, Q.B.; Sharifi, E.; Sammen, S.S.; Vojtek, M.; Linh, N.T.T. Recognition of district-wise groundwater stress zones using the GLDAS-2 catchment land surface model during lean season in the Indian state of West Bengal. *Acta Geophys.* **2021**, *69*, 175–198. [\[CrossRef\]](#)
70. Kumar, K.M.; Hanumanthappa, M.; Mavarkar, N.S.; Marimuthu, S. Review on smart practices and technologies for climate resilient agriculture. *Int. J. Curr. Microbiol. App. Sci.* **2018**, *7*, 3021–3031. [\[CrossRef\]](#)
71. Rhodes, E.; Scott, W.A. Jaccard, M. Designing flexible regulations to mitigate climate change: A cross-country comparative policy analysis. *Energy Policy* **2021**, *156*, 112419. [\[CrossRef\]](#)
72. Bremer, S.; Wardekker, A.; Dessai, S.; Sobolowski, S.; Slaattelid, R.; van der Sluijs, J. Toward a multi-faceted conception of co-production of climate services. *Clim. Serv.* **2019**, *13*, 42–50. [\[CrossRef\]](#)
73. Swim, J.; Clayton, S.; Doherty, T.; Gifford, R.; Howard, G.; Reser, J.; Weber, E. Psychology and global climate change: Addressing a multi-faceted phenomenon and set of challenges. In *A Report by the American Psychological Association's Task Force on the Interface between Psychology and Global Climate Change*; American Psychological Association: Washington, DC, USA, 2009.
74. Kharrazi, A.; Yu, Y.; Jacob, A.; Vora, N.; Fath, B.D. Redundancy, diversity, and modularity in network resilience: Applications for international trade and implications for public policy. *Curr. Res. Environ. Sustain.* **2020**, *2*, 100006. [\[CrossRef\]](#)
75. Simpson, N.P.; Shearing, C.D.; Dupont, B. 'Partial functional redundancy': An expression of household level resilience in response to climate risk. *Clim. Risk Manag.* **2020**, *28*, 100216. [\[CrossRef\]](#)
76. Ludwig, M.; Wilmes, P.; Schrader, S. Measuring soil sustainability via soil resilience. *Sci. Total Environ.* **2018**, *626*, 1484–1493. [\[CrossRef\]](#)
77. van Etten, J.; de Sousa, K.; Aguilar, A.; Barrios, M.; Coto, A.; Dell'Acqua, M.; Steinke, J. Crop variety management for climate adaptation supported by citizen science. *Proc. Natl. Acad. Sci. USA* **2019**, *116*, 4194–4199. [\[CrossRef\]](#)
78. Srivastav, A.L.; Dhyani, R.; Ranjan, M.; Madhav, S.; Sillanpää, M. Climate-resilient strategies for sustainable management of water resources and agriculture. *Environ. Sci. Pollut. Res.* **2021**, *28*, 41576–41595. [\[CrossRef\]](#)
79. Rahman, M.M.; Aravindakshan, S.; Hoque, M.A.; Rahman, M.A.; Gulandaz, M.A.; Rahman, J.; Islam, M.T. Conservation tillage (CT) for climate-smart sustainable intensification: Assessing the impact of CT on soil organic carbon accumulation, greenhouse gas emission and water footprint of wheat cultivation in Bangladesh. *Environ. Sustain. Indic.* **2021**, *10*, 100106. [\[CrossRef\]](#)
80. Borkar, N. Agricultural Mechanization for Small Holders Necessary for Climate Resilient Agriculture. In *Climate Resilient Agricultural Technologies for Future. Training Manual, Model Training Course on Climate Resilient Agricultural Technologies for Future*; ICAR-National Rice Research Institute: Cuttack, India, 2019; Volume 3, p. 64.
81. Sekaran, U.; Lai, L.; Ussiri, D.A.; Kumar, S.; Clay, S. Role of integrated crop-livestock systems in improving agriculture production and addressing food security—A review. *J. Agric. Food Res.* **2021**, *5*, 100190. [\[CrossRef\]](#)

Disclaimer/Publisher's Note: The statements, opinions and data contained in all publications are solely those of the individual author(s) and contributor(s) and not of MDPI and/or the editor(s). MDPI and/or the editor(s) disclaim responsibility for any injury to people or property resulting from any ideas, methods, instructions or products referred to in the content.